Electronic Supplementary Information (ESI)

The fold preference and thermodynamic stability of α-synuclein fibrils is encoded in the non-amyloid-β component region

Liang Xu, Shayon Bhattacharya, and Damien Thompson*

Department of Physics, Bernal Institute, University of Limerick, V94 T9PX, Ireland

Contents

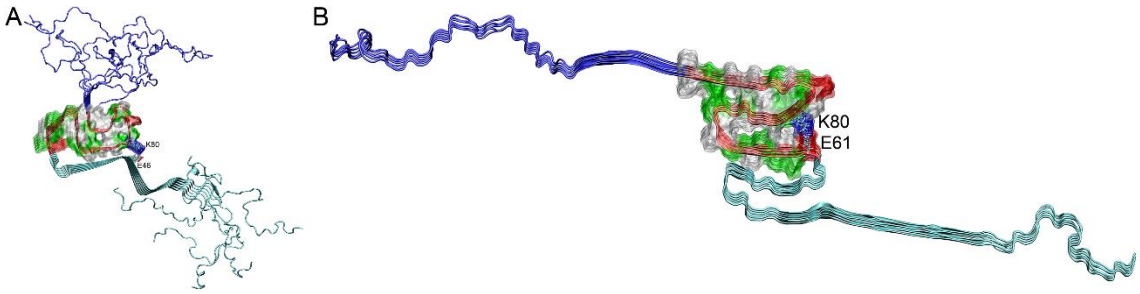

Fig. S1. The full-length of αS fibril structures in the G-Key (A) and 5Fold (B) morphology. The N-terminus (residues 1–60), the NAC region (residues 61–95), and the C-terminus (residues 96–140) are colored in cyan, red, and blue, respectively. The NAC region is also highlighted by a transparent space-filling surface. A salt bridge is formed between Glu^{46} and Lys^{80} in the G-Key fibril, and between Glu^{61} and Lys^{80} in the 5Fold fibril, respectively, as indicated. The full-length of αS fibril structure in the G-Key was taken from the PDB database (PDB ID: 2N0A). The full-length of αS fibril structure in the 5Fold was constructed based on our previous study of αS(20–110) fibril model (*Eur. J. Med. Chem*. **2016**, 121, 841).

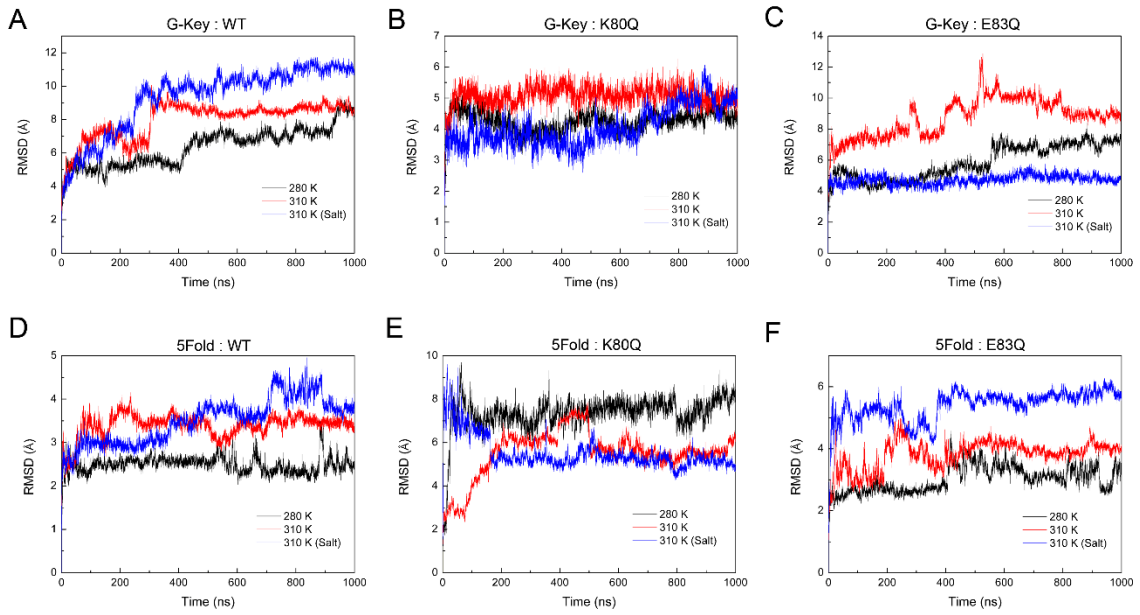

Fig. S2. Root-mean-square deviations (RMSD) of backbone atoms of NAC fibril structures.

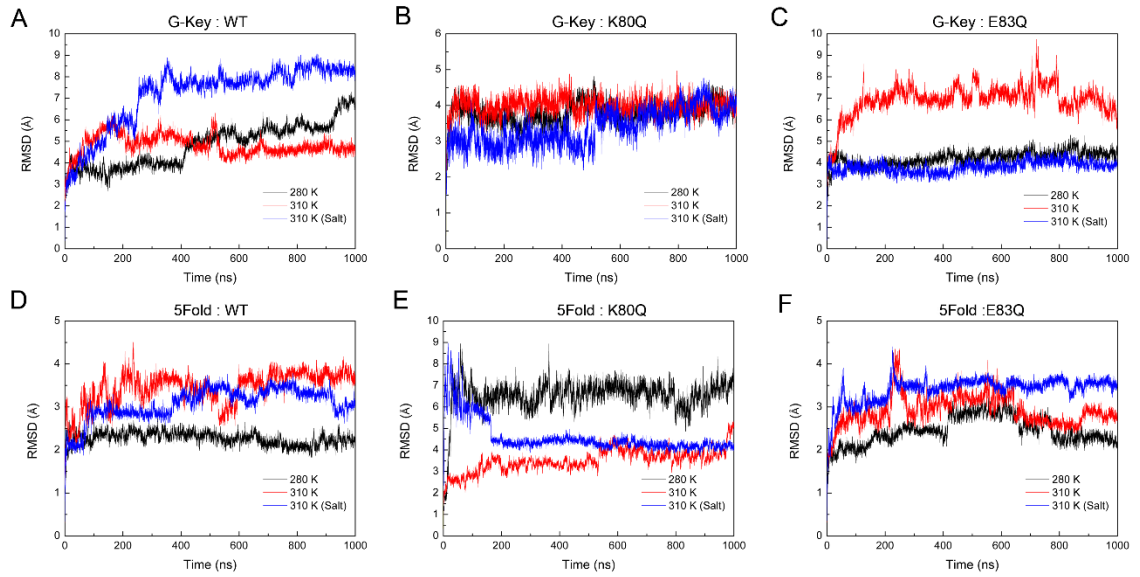

Fig. S3. Root-mean-square deviations (RMSD) of backbone atoms of NAC fibril structures excluding end monomers.

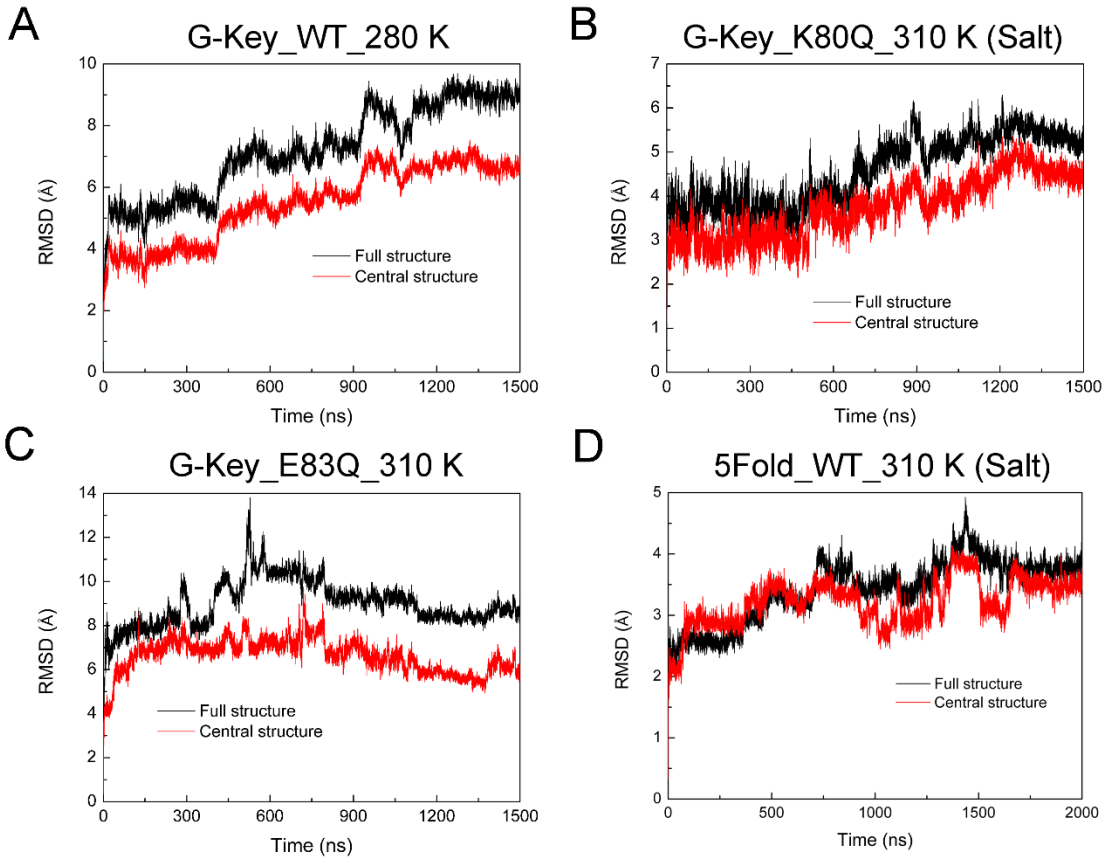

Fig. S4. Root-mean-square deviations (RMSD) of backbone atoms of NAC fibril structures, and NAC central structures (excluding end monomers) for different systems.

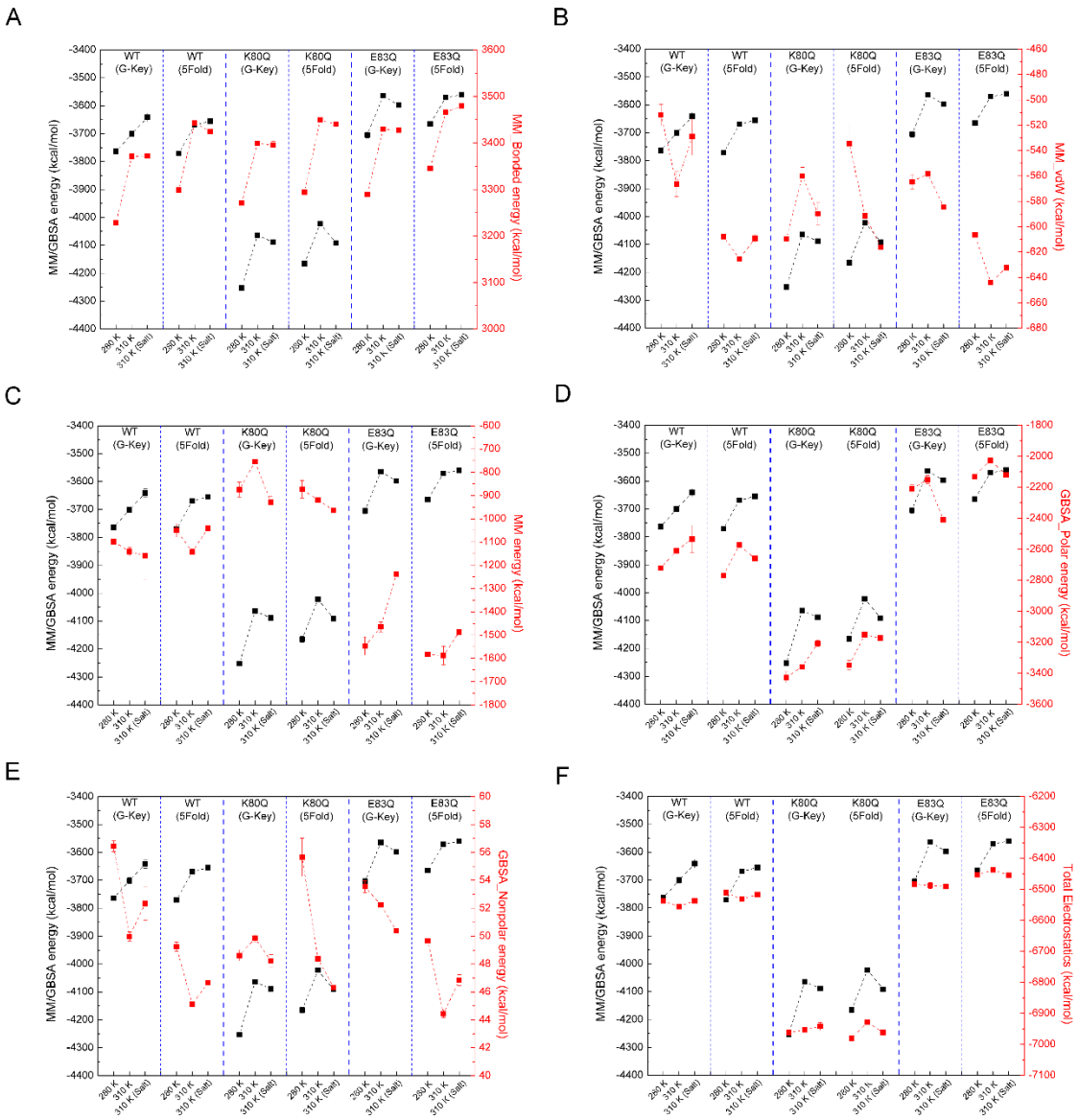

Fig. S5. The relation between conformational energy (MM/GBSA energy) and its individual contributions. (A) MM/GBSA and MM bonded energy, with a Pearson correlation coefficient (P.C.C. = 0.32); (B) MM/GBSA and MM van der Waals energy, with a Pearson correlation coefficient (P.C.C. = –0.12); (C) MM/GBSA and MM energy, with a Pearson correlation coefficient (P.C.C. = –0.79); (D) MM/GBSA and Polar contribution of GBSA solvation energy, with a Pearson correlation coefficient (P.C.C. = 0.94); (E) MM/GBSA and Nonpolar energy of GBSA solvation energy, with a Pearson correlation coefficient (P.C.C. = –0.09); (F) MM/GBSA and total electrostatic energy (sum of MM electrostatic and GBSA polar solvation energy), with a Pearson correlation coefficient (P.C.C. = 0.97);

Fig. S6. Population of in-register HBs in each model (pages S6–S30).

G-Key_WT_280 K

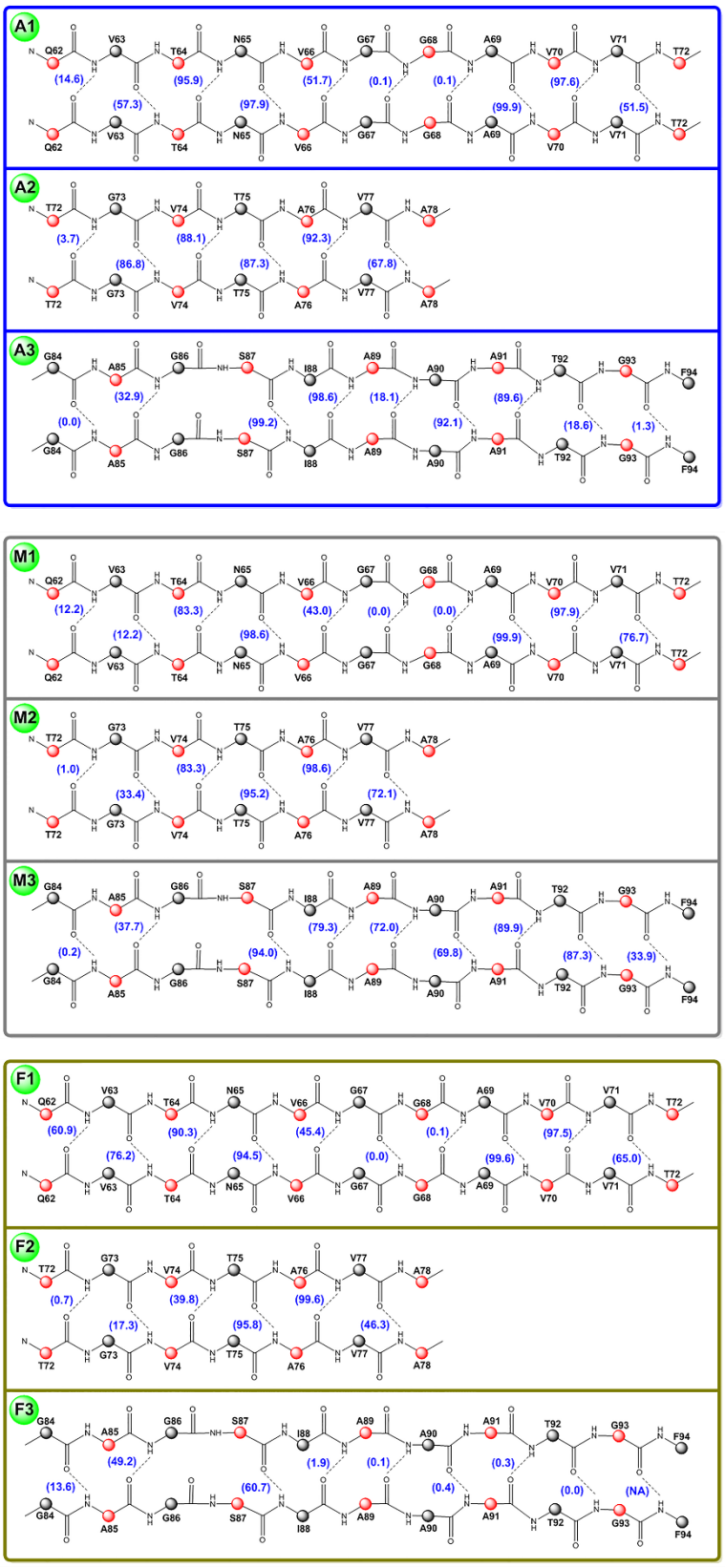
A1
Q62 V63 T64 N65 V66 G67 G68 A69 V70 V71 T72
(14.6) (95.9) (51.7) (0.1) (0.1) (97.6)
(57.3) (97.9) (99.9) (51.5)
A2
T72 G73 V74 T75 A76 V77 A78
(3.7) (88.1) (92.3)
(86.8) (87.3) (67.8)
A3
G84 A85 G86 S87 I88 A89 A90 A91 T92 G93 F94
(32.9) (98.6) (18.1) (89.6)
(0.0) (99.2) (92.1) (18.6) (1.3)
M1
Q62 V63 T64 N65 V66 G67 G68 A69 V70 V71 T72
(12.2) (83.3) (43.0) (0.0) (0.0) (97.9)
(12.2) (98.6) (99.9) (76.7)
M2
T72 G73 V74 T75 A76 V77 A78
(1.0) (83.3) (98.6)
(33.4) (95.2) (72.1)
M3
G84 A85 G86 S87 I88 A89 A90 A91 T92 G93 F94
(37.7) (79.3) (72.0) (89.9)
(0.2) (94.0) (69.8) (87.3) (33.9)
F1
Q62 V63 T64 N65 V66 G67 G68 A69 V70 V71 T72
(60.9) (90.3) (45.4) (0.1) (97.5)
(76.2) (94.5) (0.0) (99.6) (65.0)
F2
T72 G73 V74 T75 A76 V77 A78
(0.7) (39.8) (99.6)
(17.3) (95.8) (46.3)
F3
G84 A85 G86 S87 I88 A89 A90 A91 T92 G93 F94
(49.2) (1.9) (0.1) (0.3)
(13.6) (60.7) (0.4) (0.0) (NA)

G-Key_WT_310 K

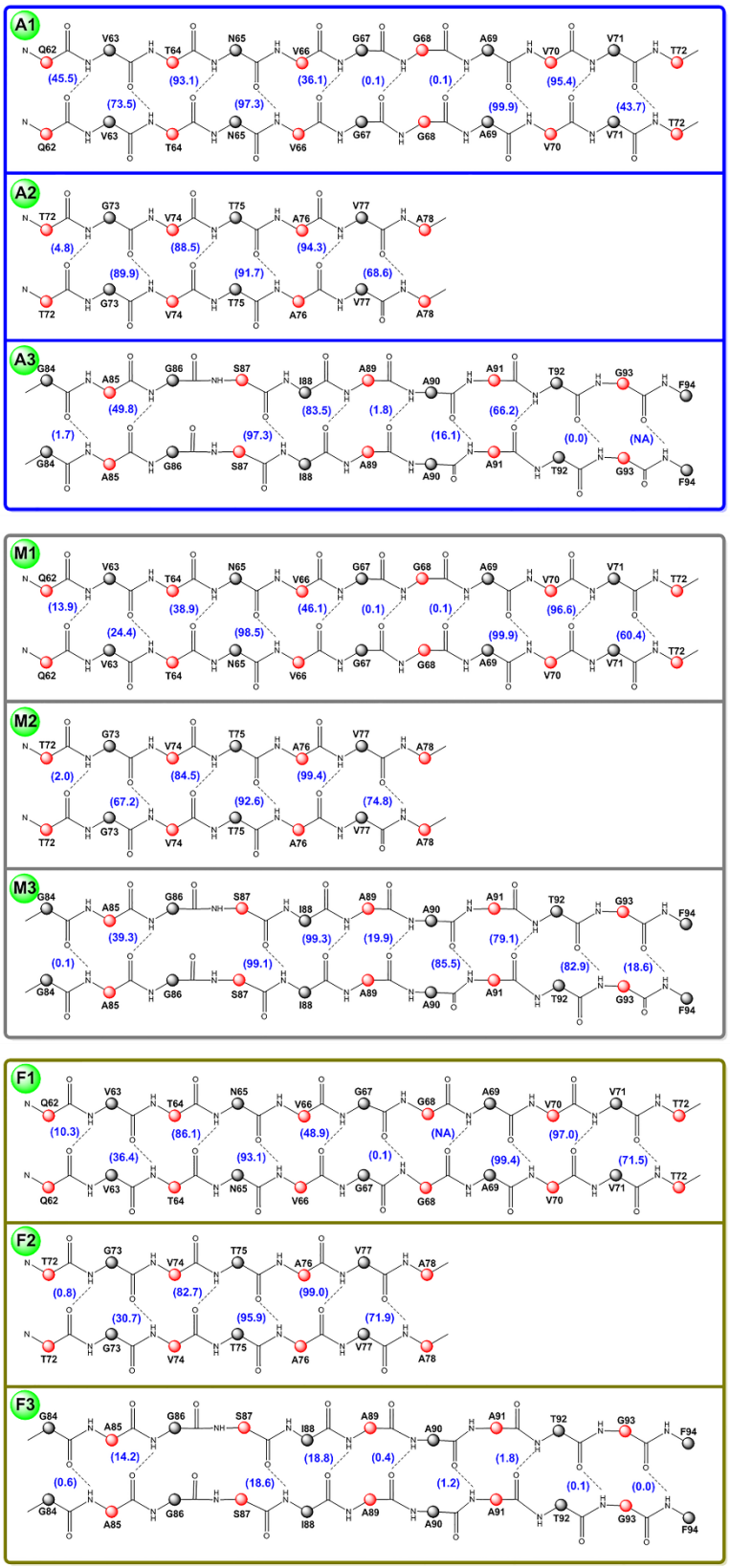
A1
Q62 V63 T64 N65 V66 G67 G68 A69 V70 V71 T72
(45.5) (93.1) (36.1) (0.1) (0.1) (95.4)
(73.5) (97.3) (99.9) (43.7)
A2
T72 G73 V74 T75 A76 V77 A78
(4.8) (88.5) (94.3)
(89.9) (91.7) (68.6)
A3
G84 A85 G86 S87 I88 A89 A90 A91 T92 G93 F94
(49.8) (83.5) (1.8) (66.2)
(1.7) (97.3) (16.1) (0.0) (NA)
M1
Q62 V63 T64 N65 V66 G67 G68 A69 V70 V71 T72
(13.9) (38.9) (46.1) (0.1) (0.1) (96.6)
(24.4) (98.5) (99.9) (60.4)
M2
T72 G73 V74 T75 A76 V77 A78
(2.0) (84.5) (99.4)
(67.2) (92.6) (74.8)
M3
G84 A85 G86 S87 I88 A89 A90 A91 T92 G93 F94
(39.3) (99.3) (19.9) (79.1)
(0.1) (99.1) (85.5) (82.9) (18.6)
F1
Q62 V63 T64 N65 V66 G67 G68 A69 V70 V71 T72
(10.3) (86.1) (48.9) (NA) (97.0)
(36.4) (93.1) (0.1) (99.4) (71.5)
F2
T72 G73 V74 T75 A76 V77 A78
(0.8) (82.7) (99.0)
(30.7) (95.9) (71.9)
F3
G84 A85 G86 S87 I88 A89 A90 A91 T92 G93 F94
(14.2) (18.8) (0.4) (1.8)
(0.6) (18.6) (1.2) (0.1) (0.0)

G-Key_WT_310 K (0.15 M NaCl)

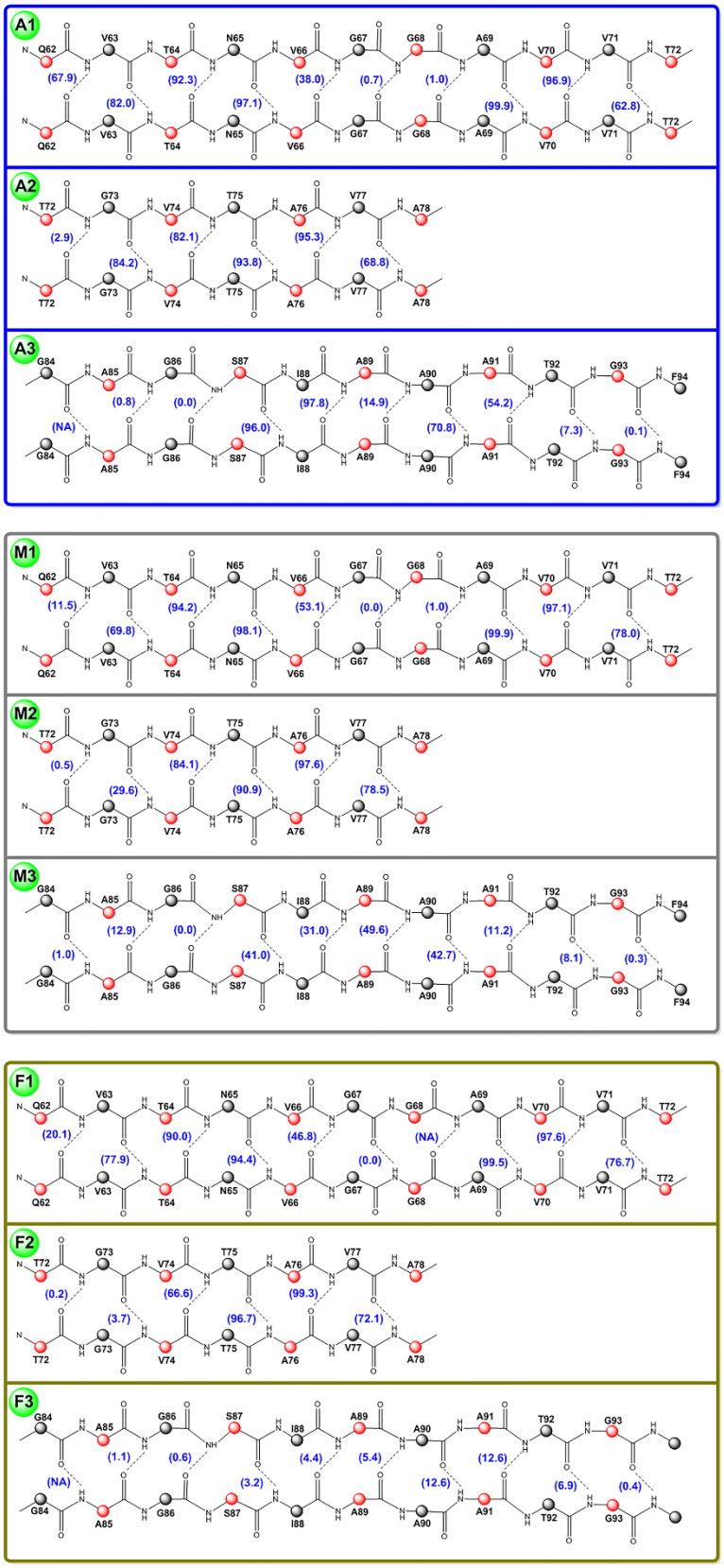

G-Key_WT_373 K

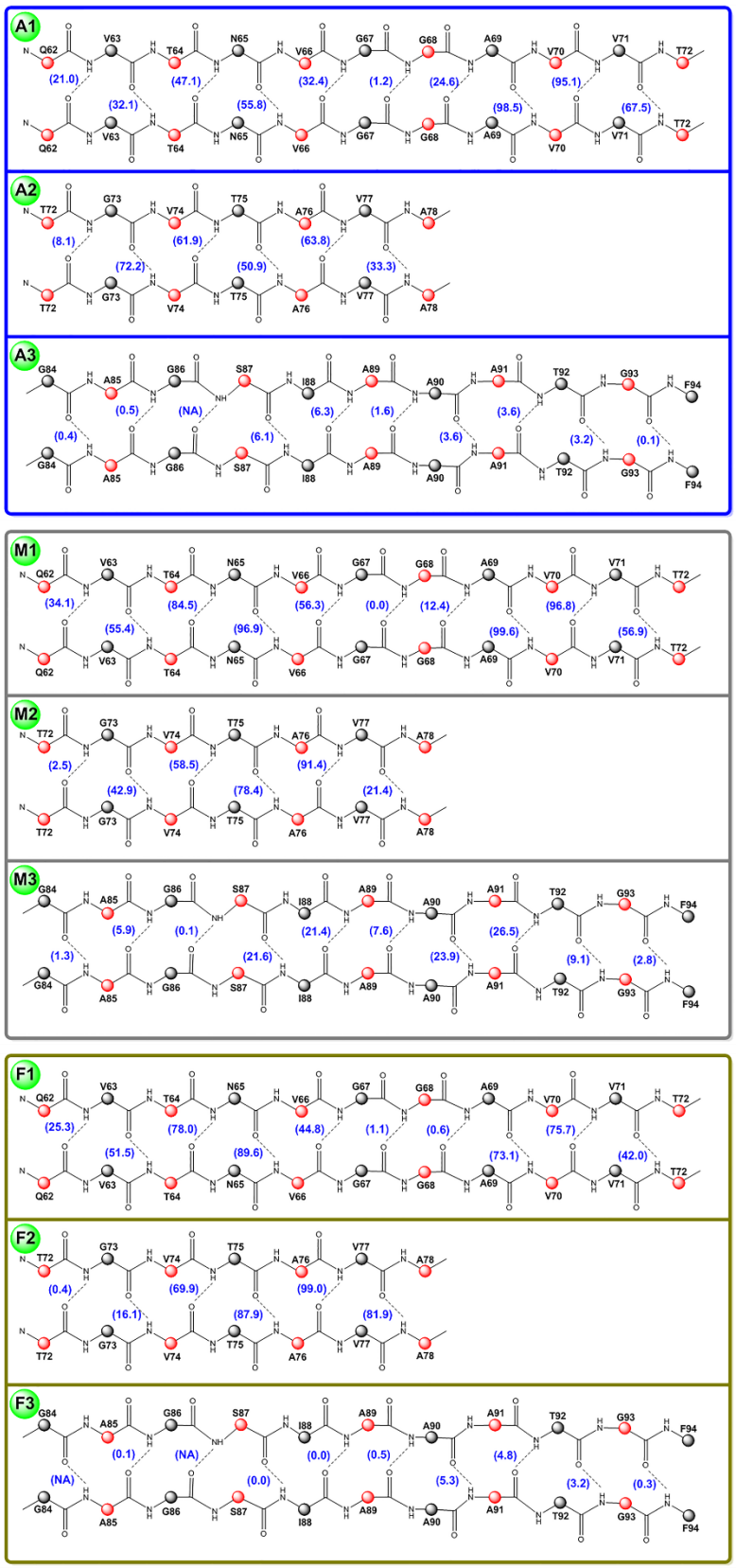
A1
Q62 V63 T64 N65 V66 G67 G68 A69 V70 V71 T72
(21.0) (47.1) (32.4) (1.2) (24.6) (95.1)
(32.1) (55.8) (98.5) (67.5)
A2
T72 G73 V74 T75 A76 V77 A78
(8.1) (61.9) (63.8)
(72.2) (50.9) (33.3)
A3
G84 A85 G86 S87 I88 A89 A90 A91 T92 G93 F94
(0.5) (NA) (6.3) (1.6) (3.6)
(0.4) (6.1) (3.6) (3.2) (0.1)
M1
Q62 V63 T64 N65 V66 G67 G68 A69 V70 V71 T72
(34.1) (84.5) (56.3) (0.0) (12.4) (96.8)
(55.4) (96.9) (99.6) (56.9)
M2
T72 G73 V74 T75 A76 V77 A78
(2.5) (58.5) (91.4)
(42.9) (78.4) (21.4)
M3
G84 A85 G86 S87 I88 A89 A90 A91 T92 G93 F94
(5.9) (0.1) (21.4) (7.6) (26.5)
(1.3) (21.6) (23.9) (9.1) (2.8)
F1
Q62 V63 T64 N65 V66 G67 G68 A69 V70 V71 T72
(25.3) (78.0) (44.8) (1.1) (0.6) (75.7)
(51.5) (89.6) (73.1) (42.0)
F2
T72 G73 V74 T75 A76 V77 A78
(0.4) (69.9) (99.0)
(16.1) (87.9) (81.9)
F3
G84 A85 G86 S87 I88 A89 A90 A91 T92 G93 F94
(0.1) (NA) (0.0) (0.5) (4.8)
(NA) (0.0) (5.3) (3.2) (0.3)

G-Key_K80Q_280 K

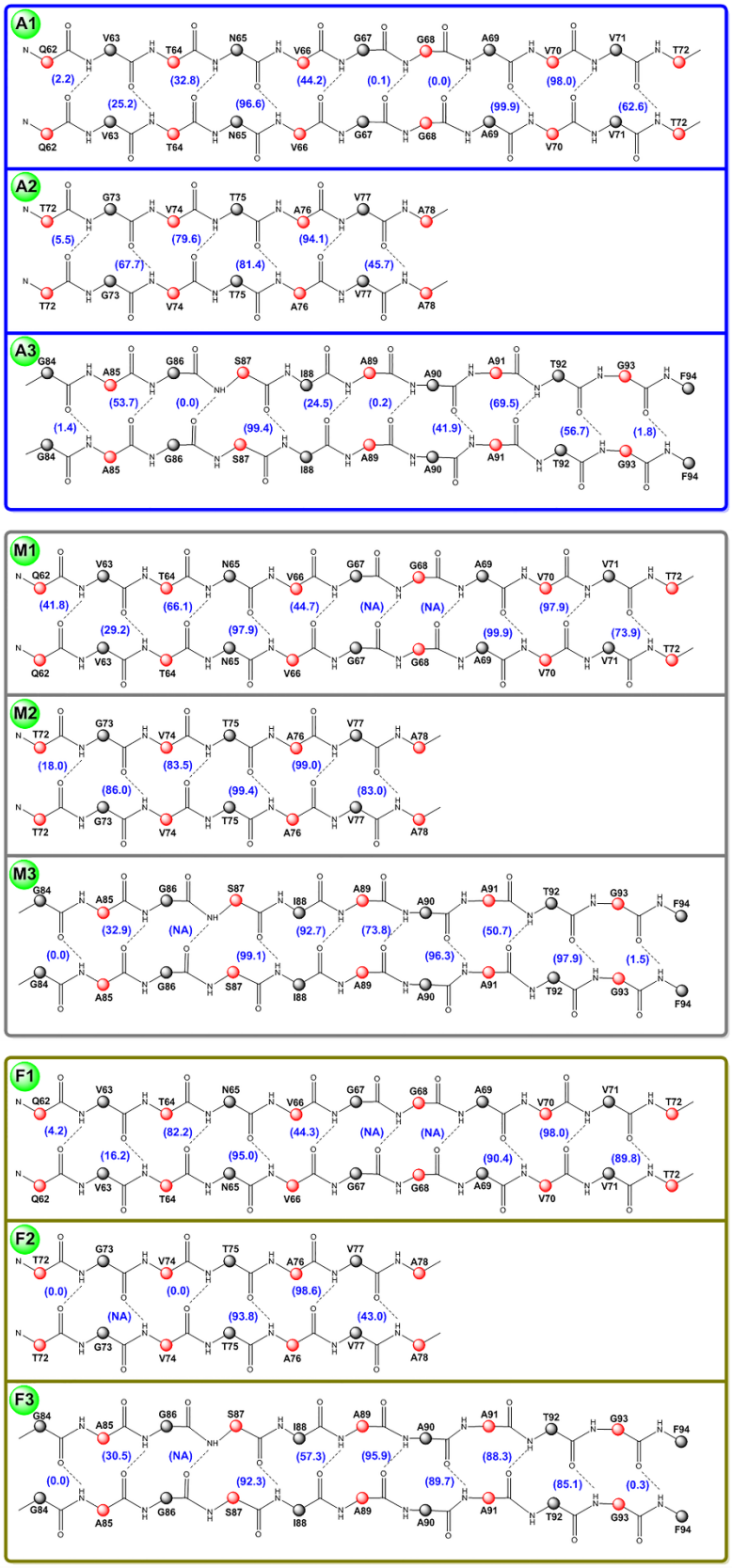

G-Key_K80Q_310 K

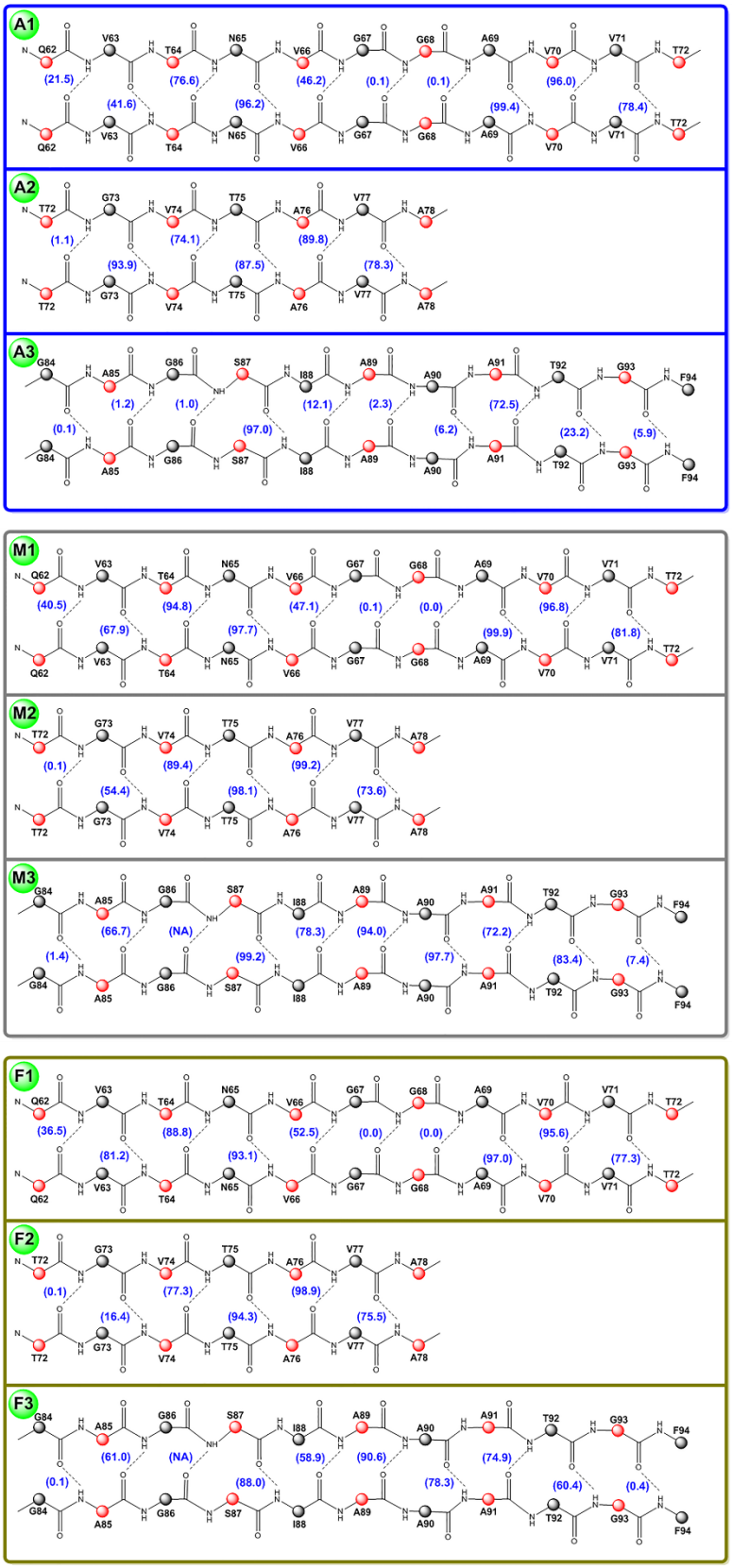

G-Key_K80Q_310 K (0.15 M NaCl)

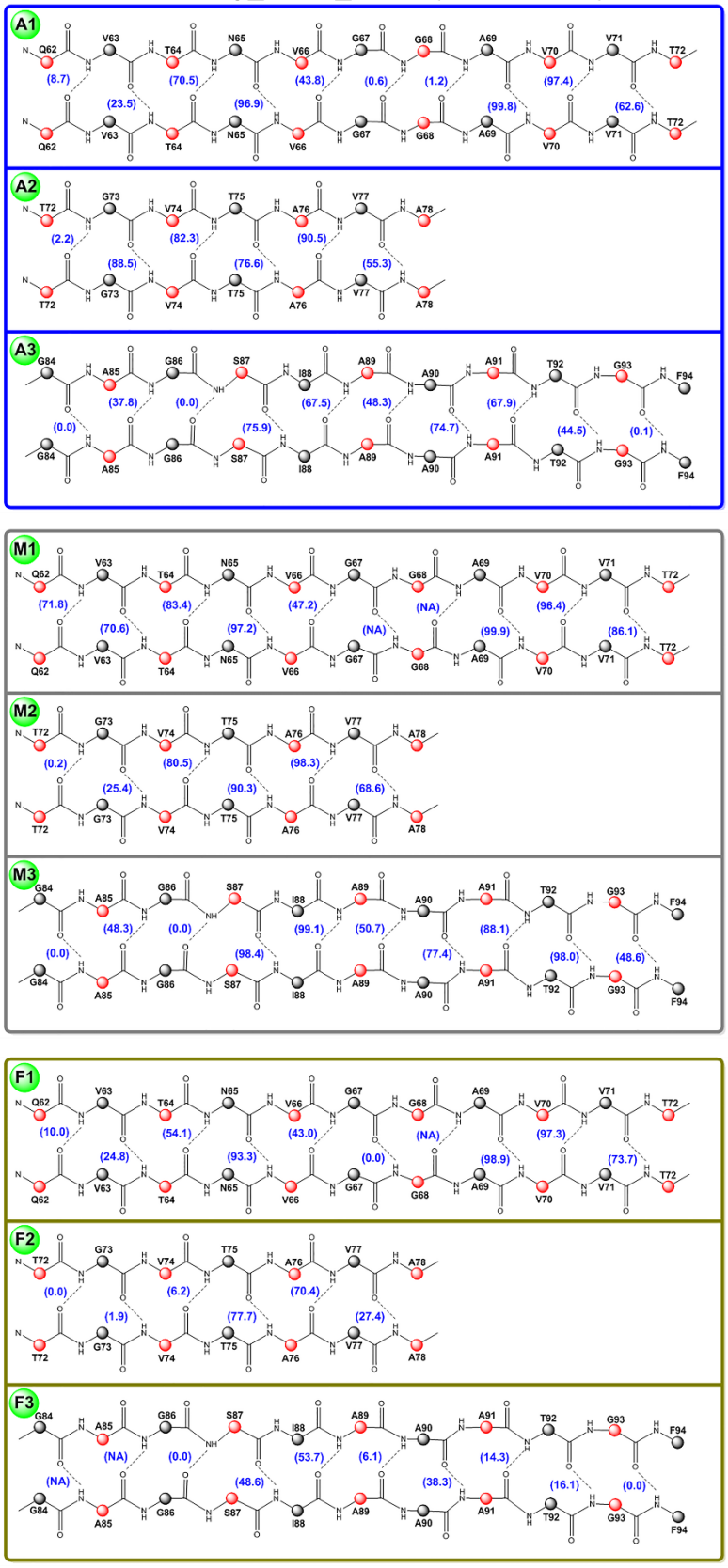

G-Key_K80Q_373 K

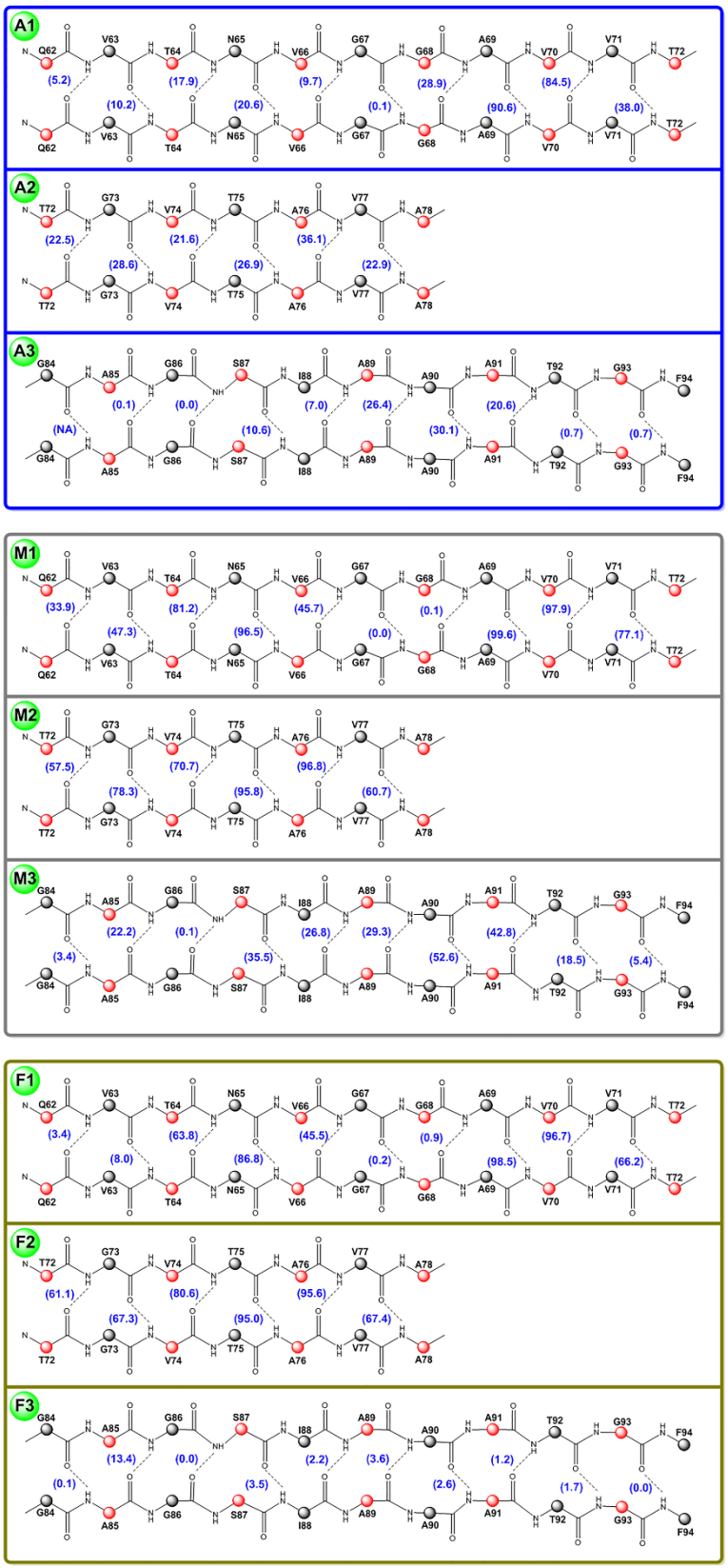

G-Key_E83Q_280 K

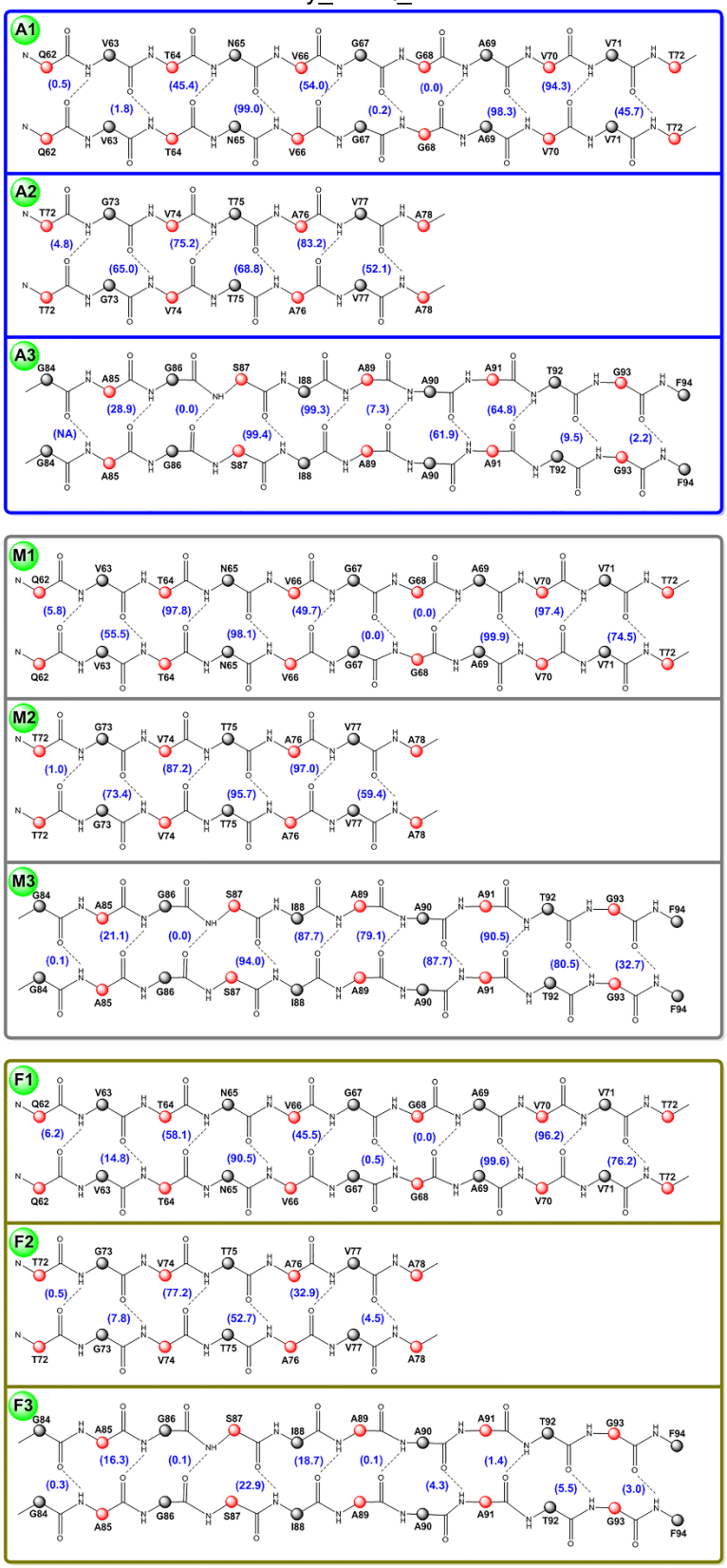

G-Key_E83Q_310 K

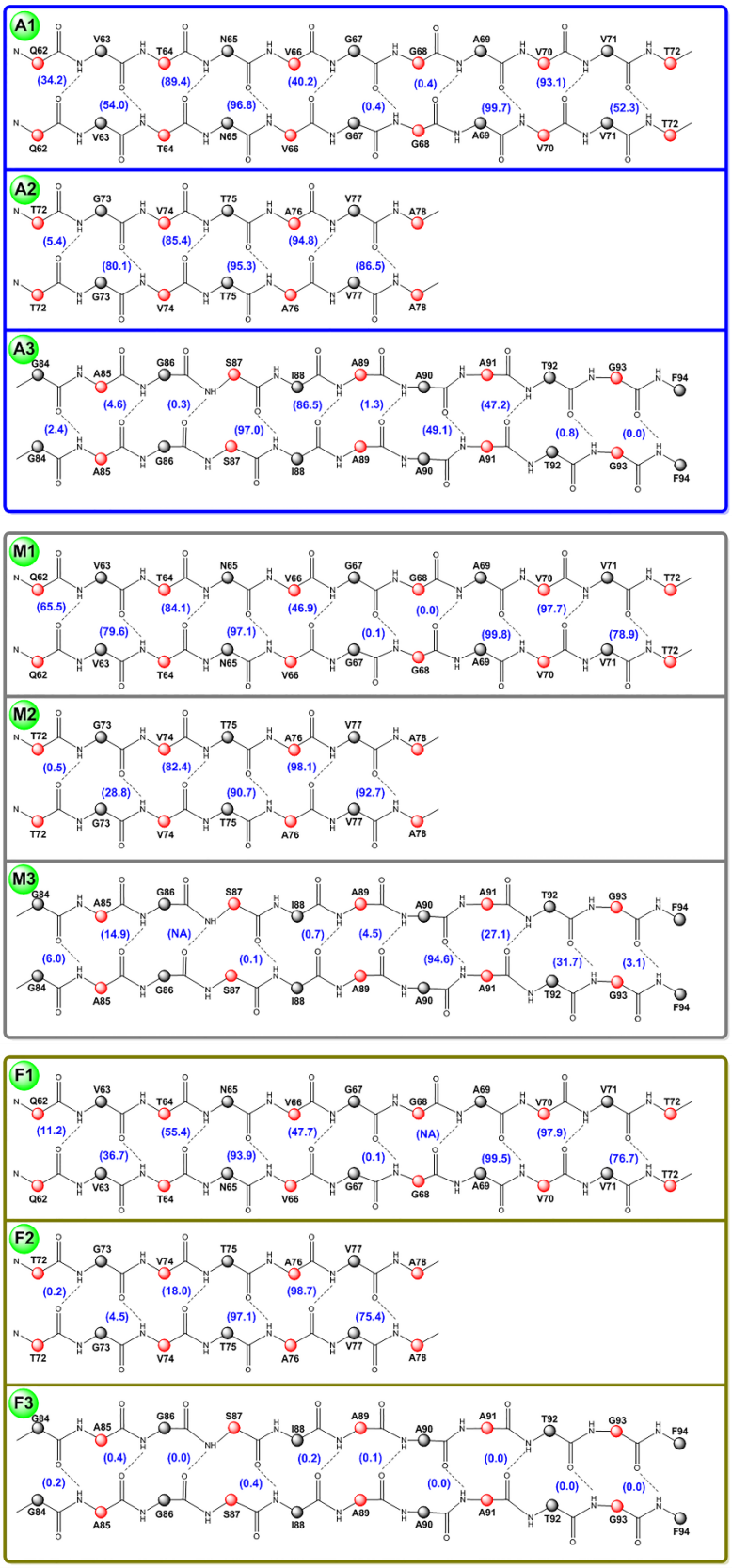

G-Key_E83Q_310 K (0.15 M NaCl)

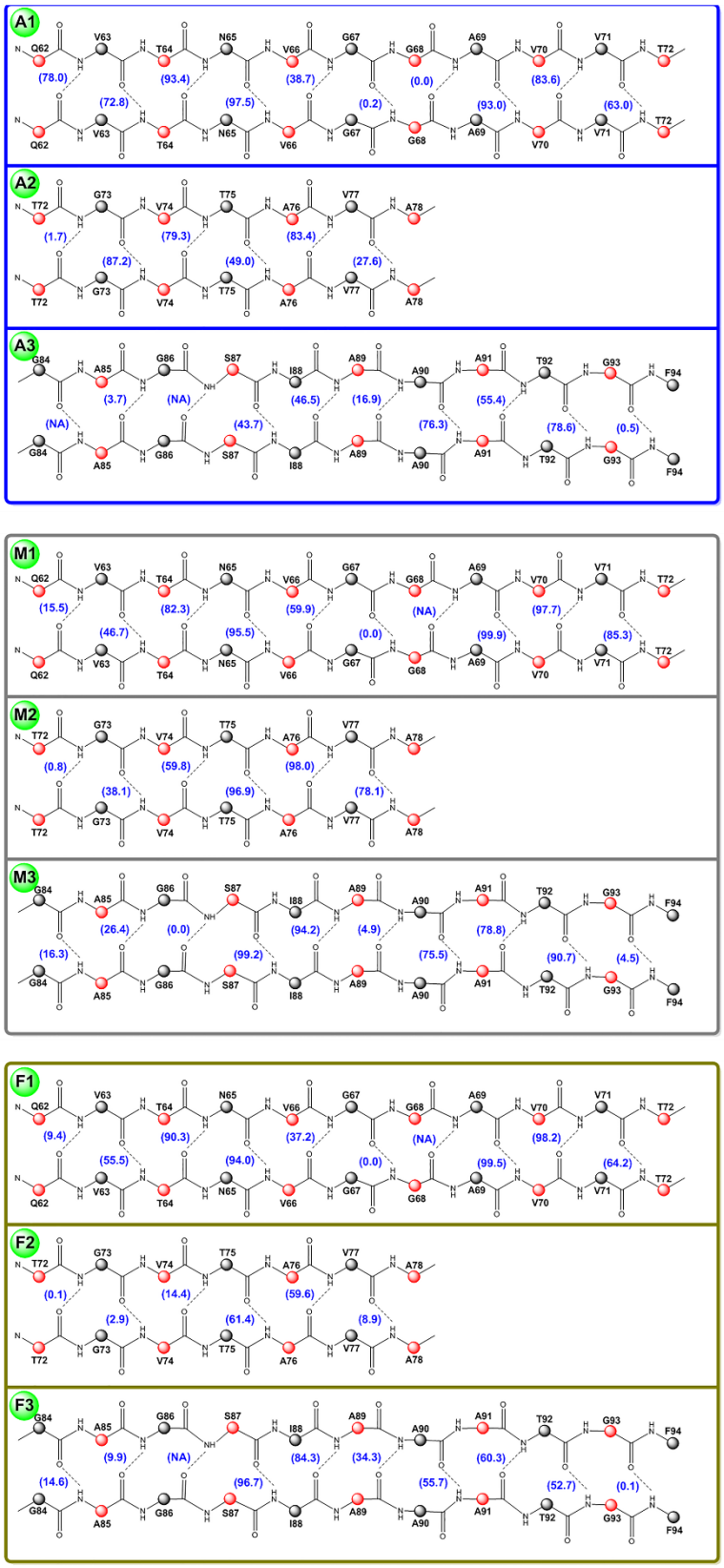

G-Key_E83Q_373 K

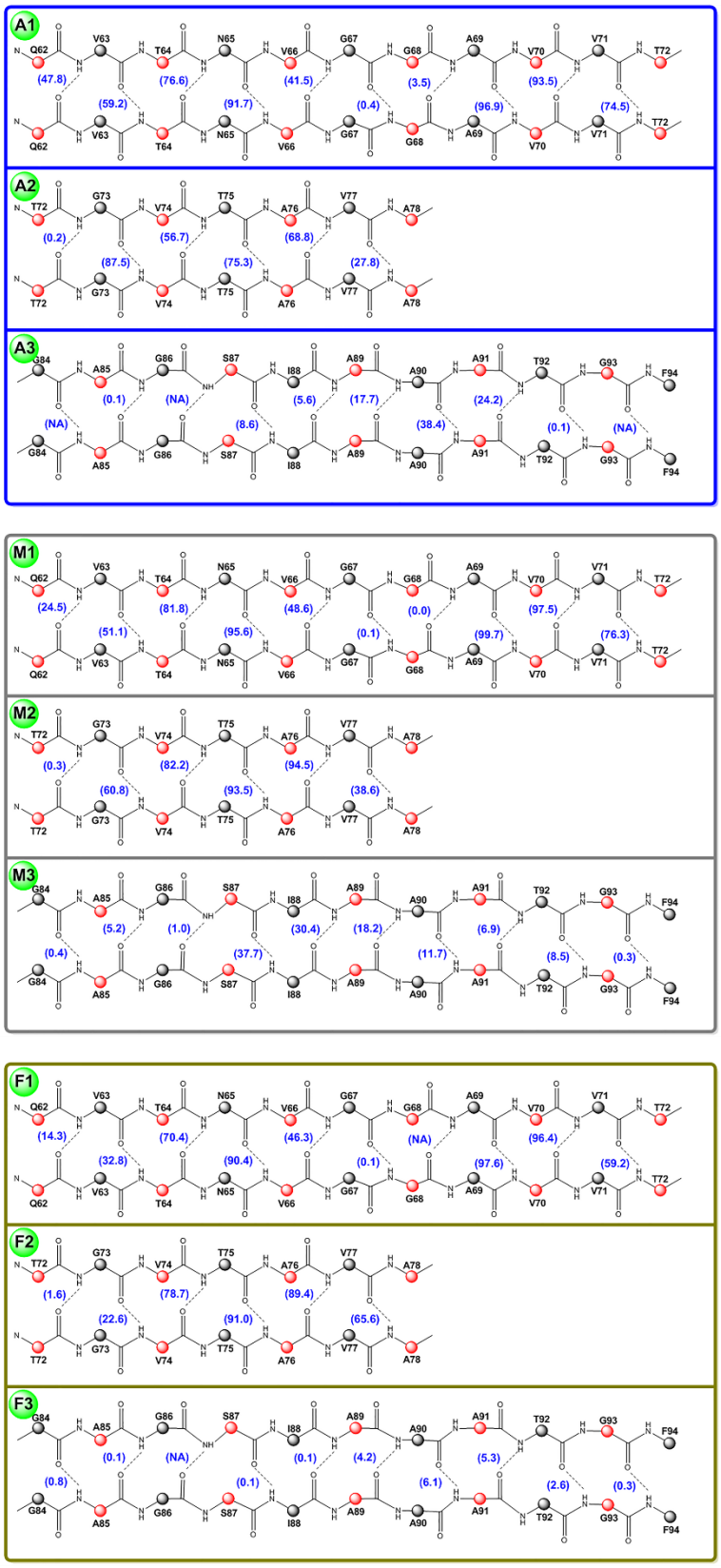

5Fold_WT_280 K

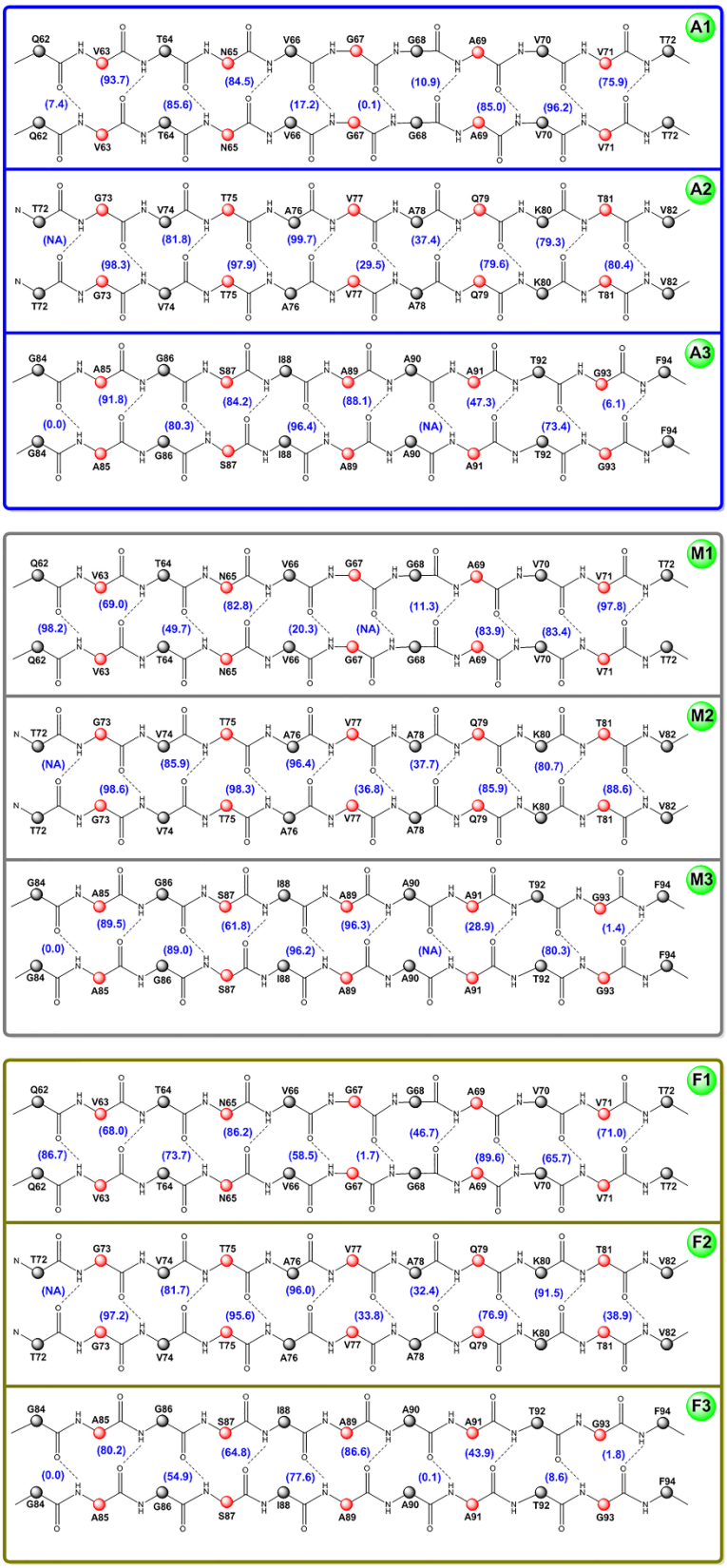

5Fold_WT_310 K

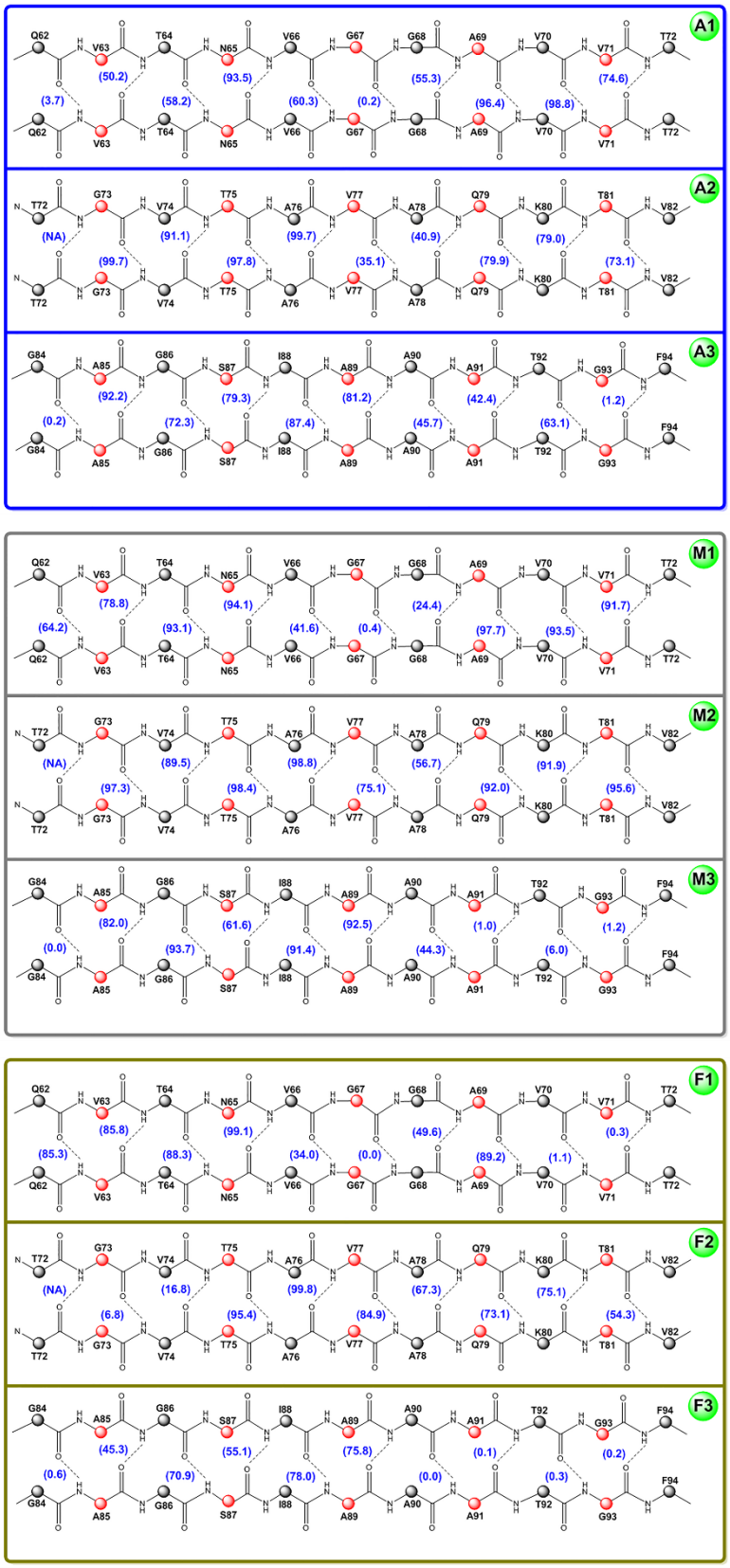

5Fold_WT_310 K (0.15 M NaCl)

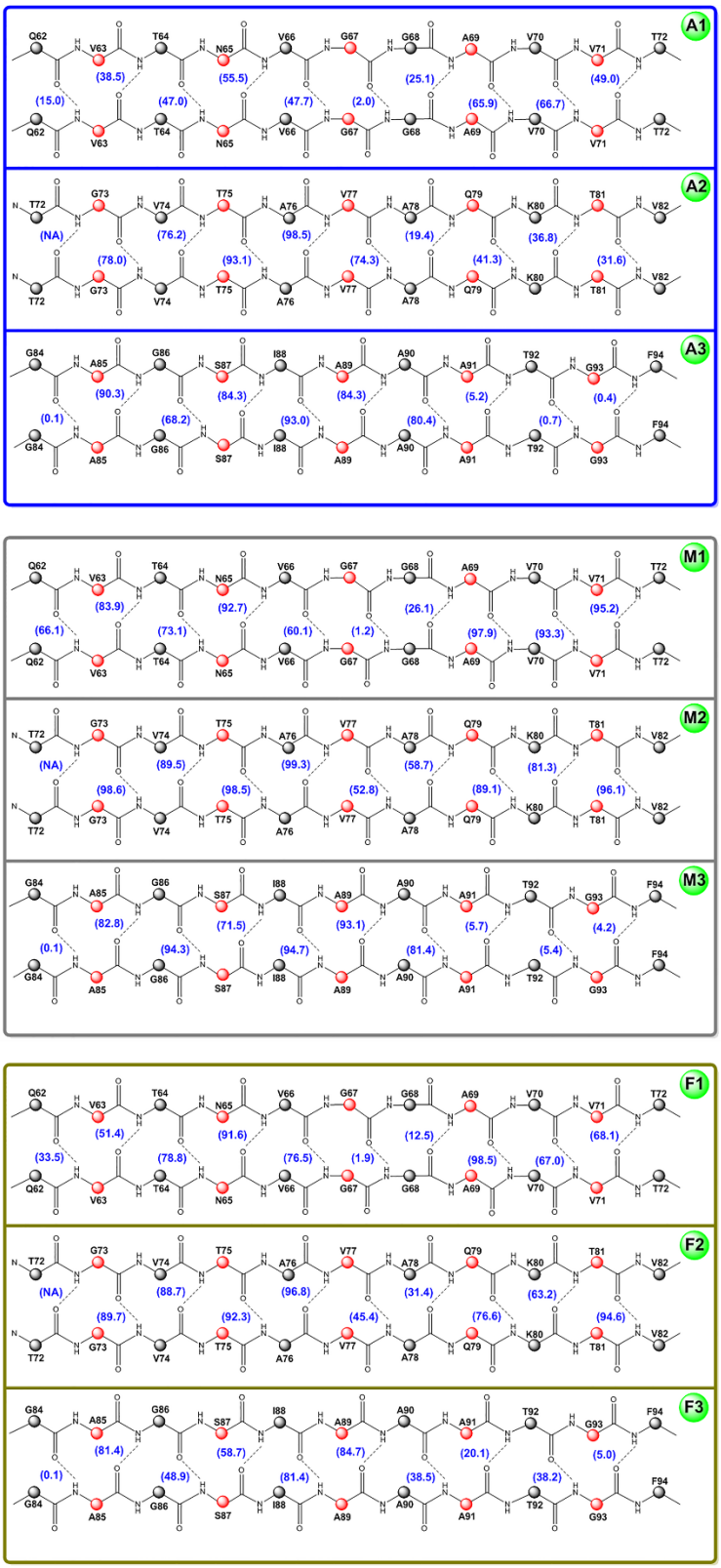

5Fold_WT_373 K

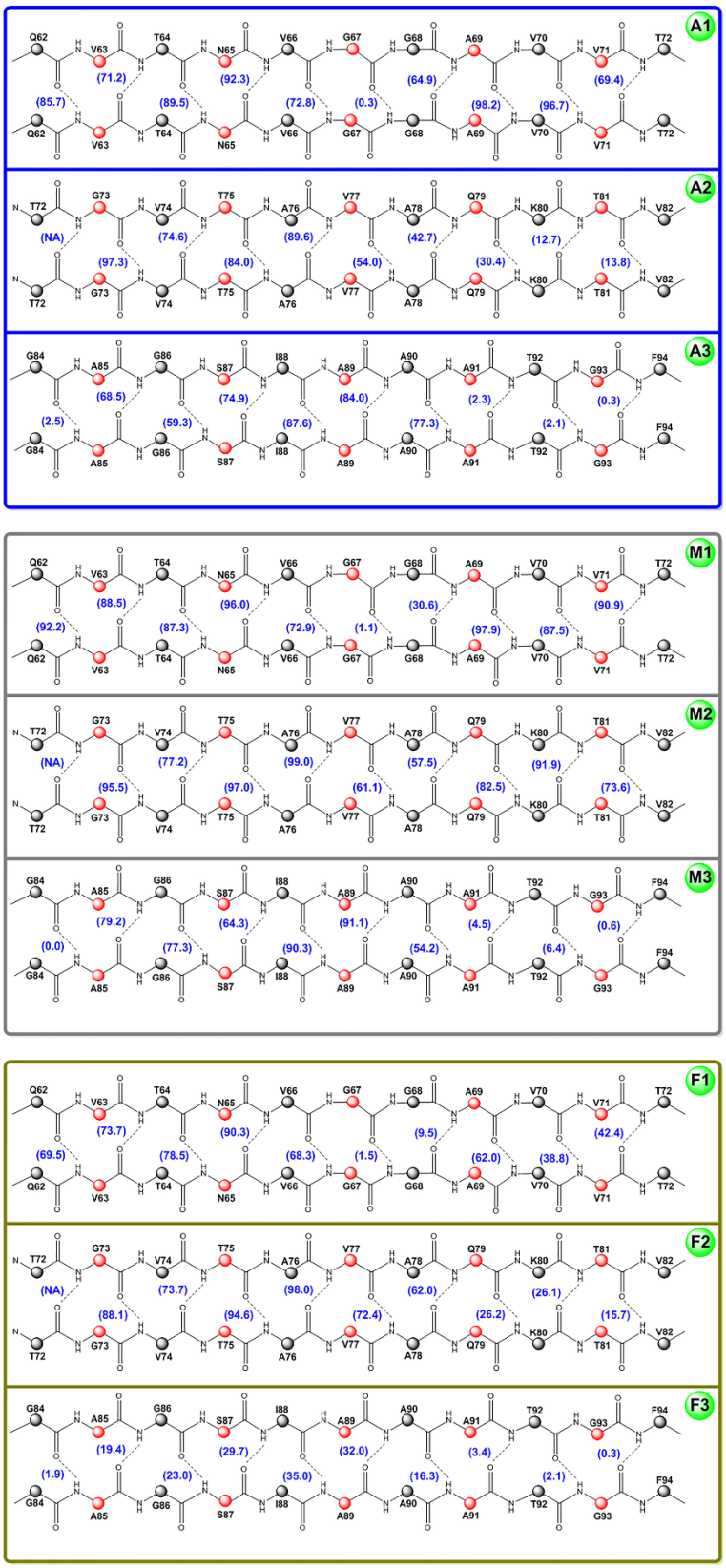

5Fold_K80Q_280 K

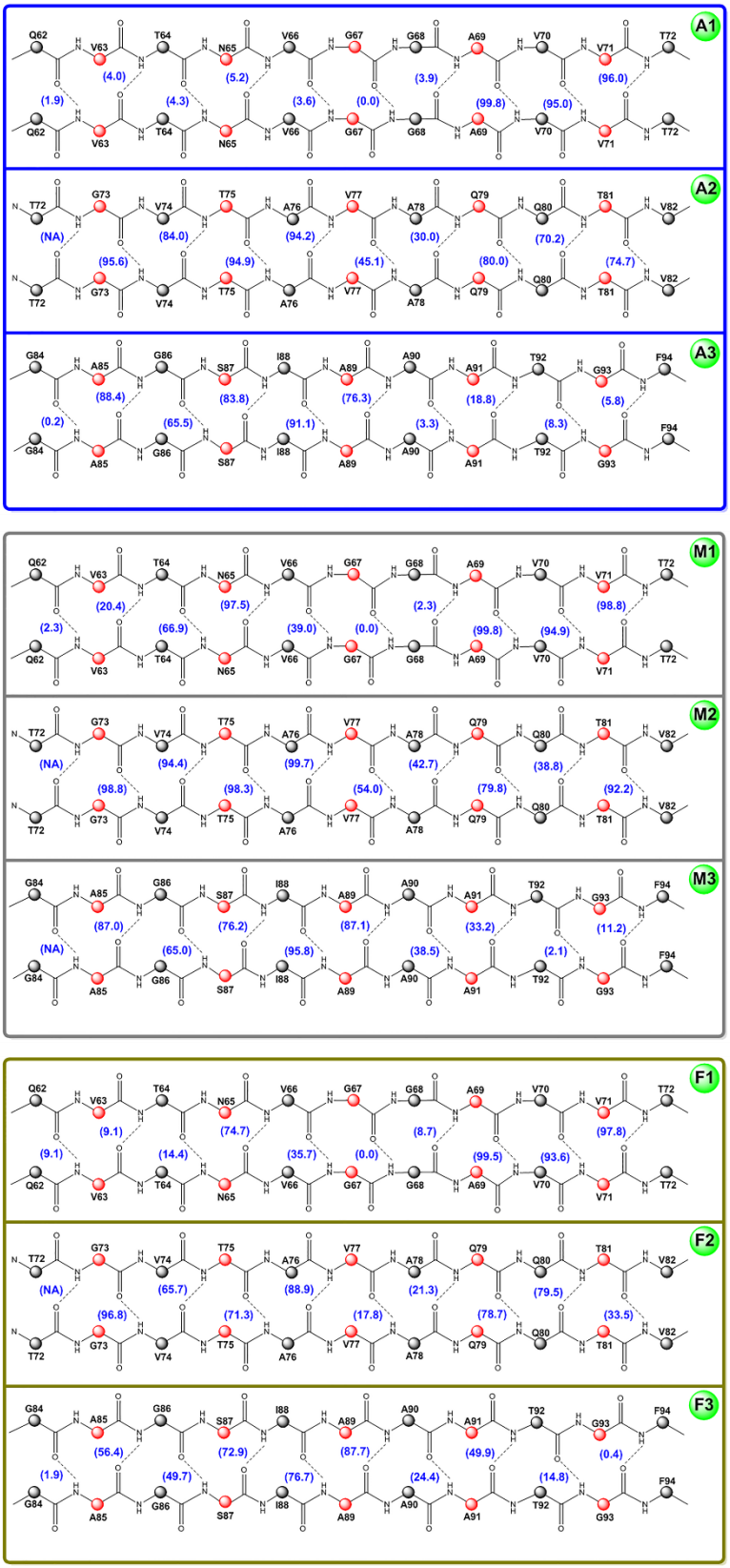

5Fold_K80Q_310 K

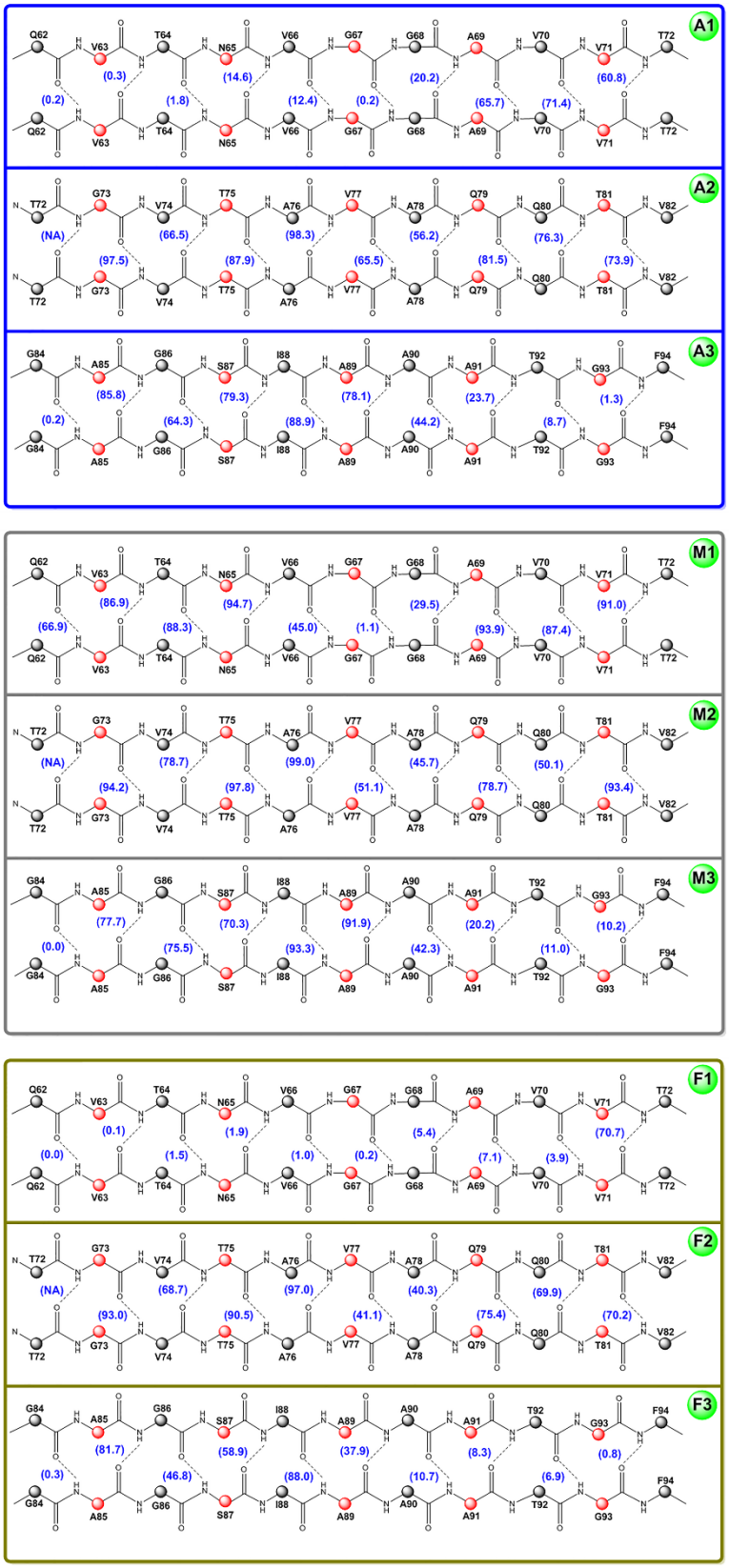

5Fold_K80Q_310 K (0.15 M NaCl)

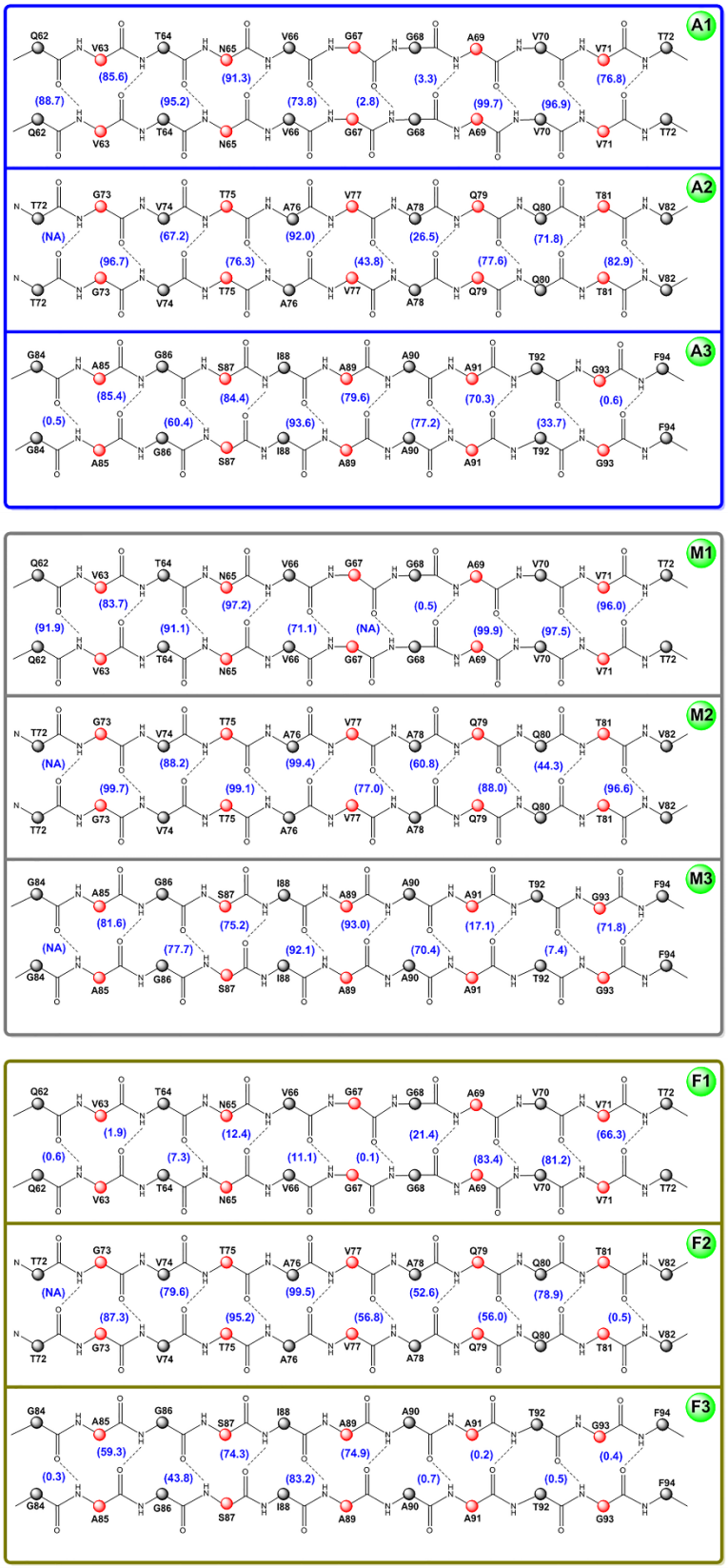

5Fold_K80Q_373 K

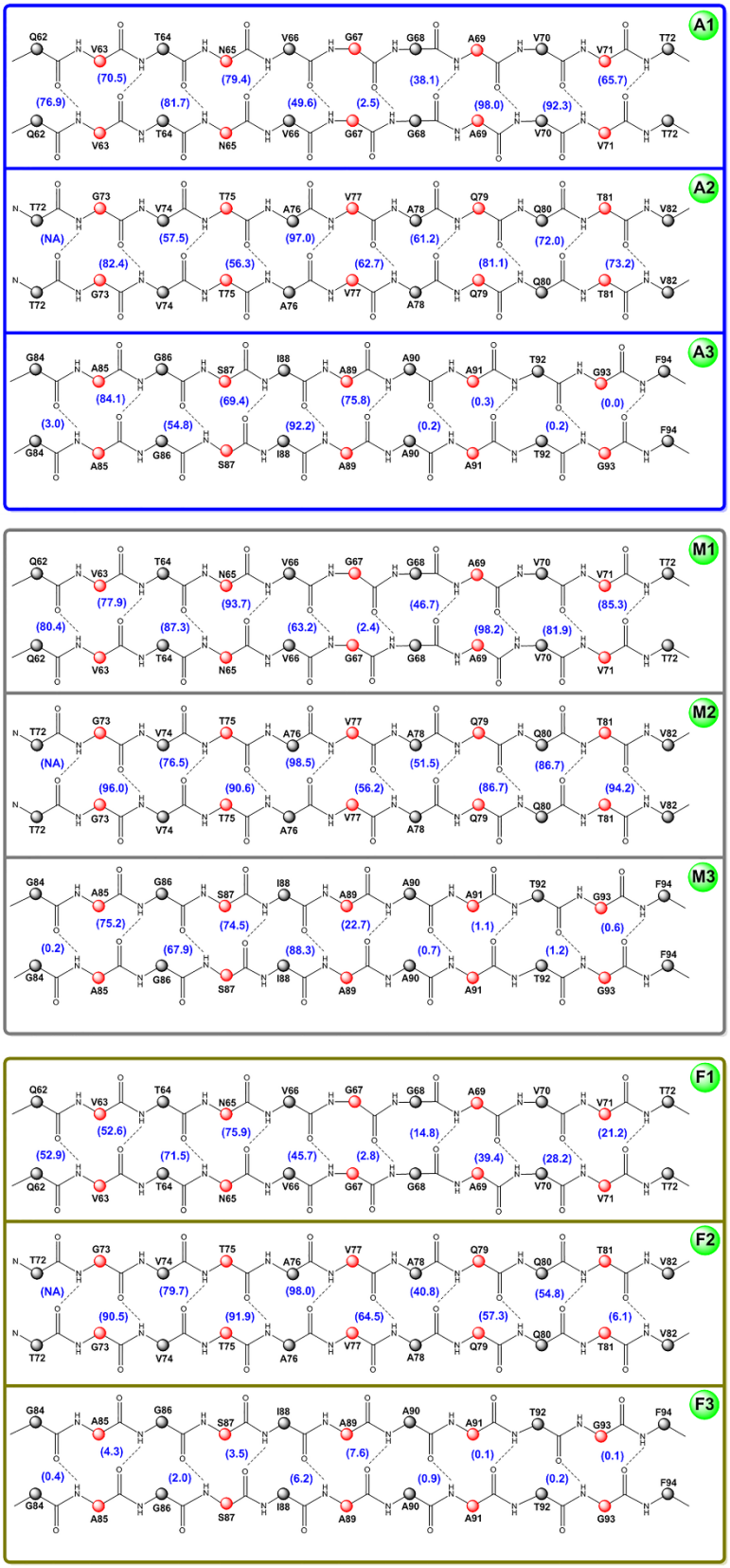

5Fold_E83Q_280 K

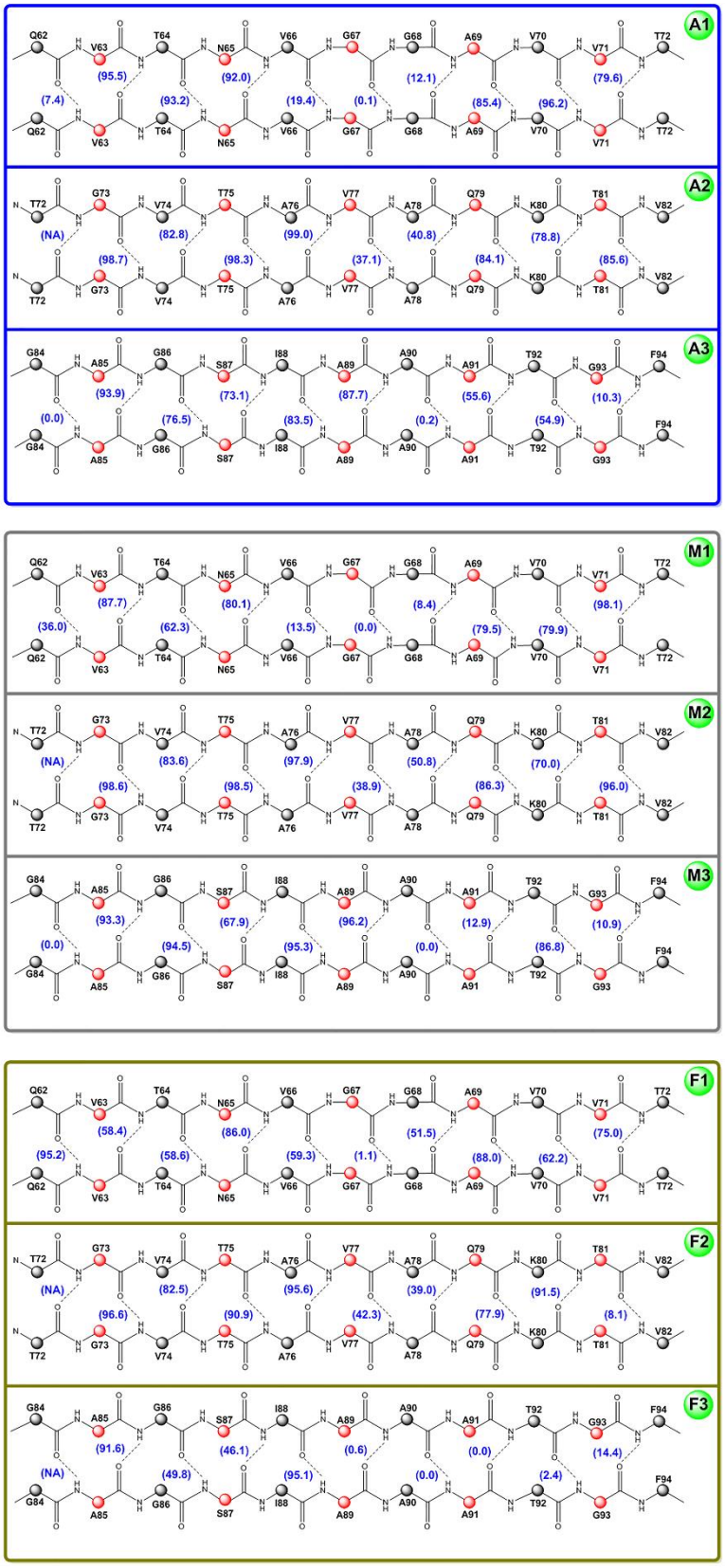

5Fold_E83Q_310 K

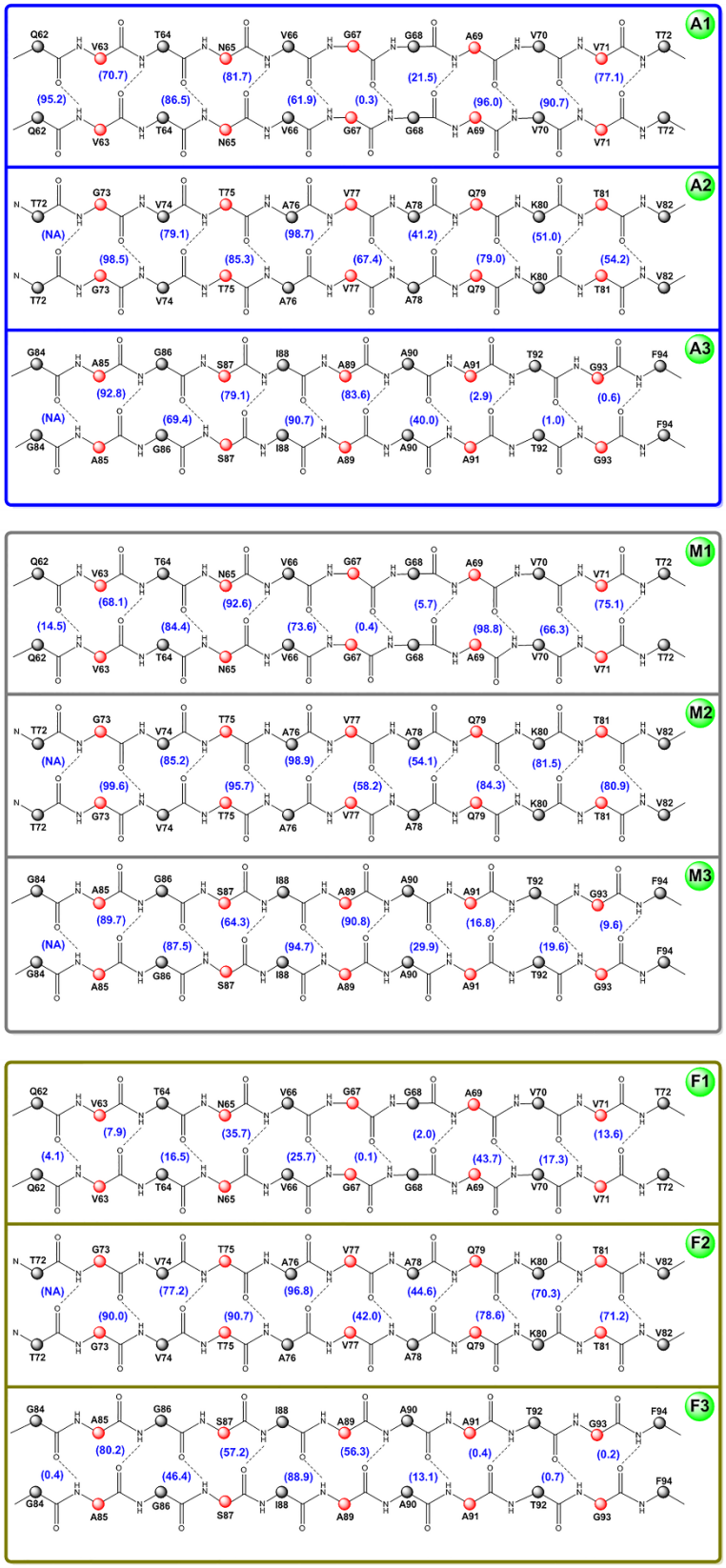

5Fold_E83Q_310 K (0.15 M NaCl)

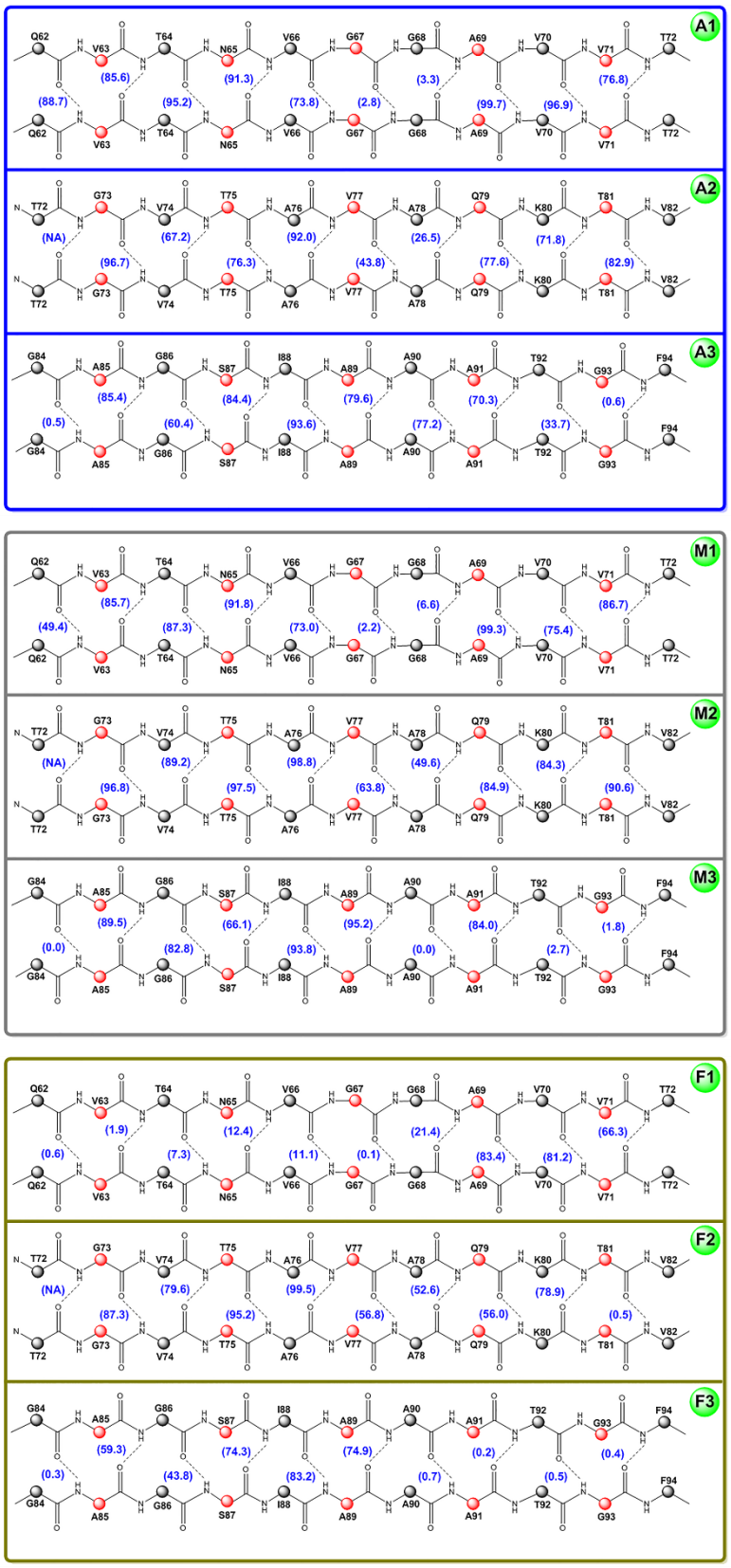

5Fold_E83Q_373 K

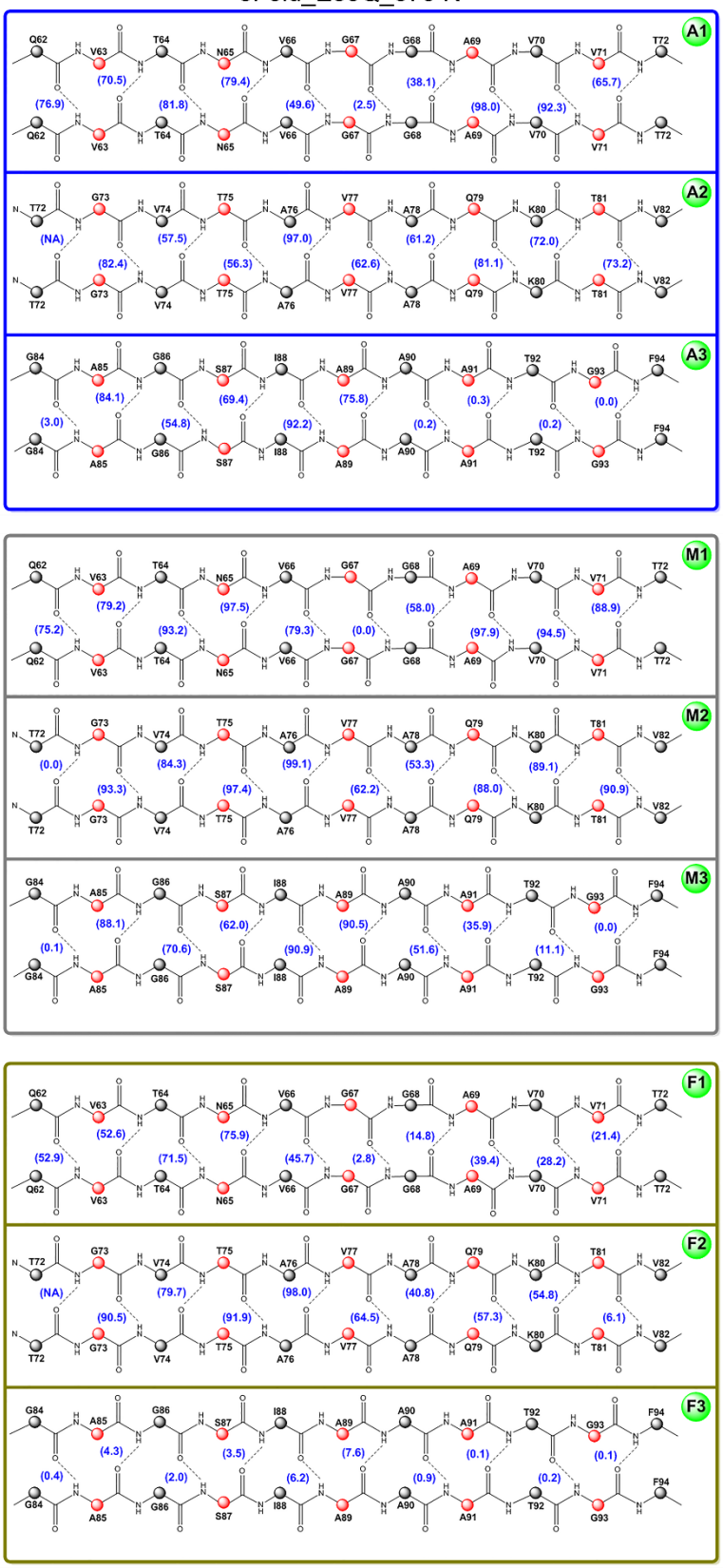

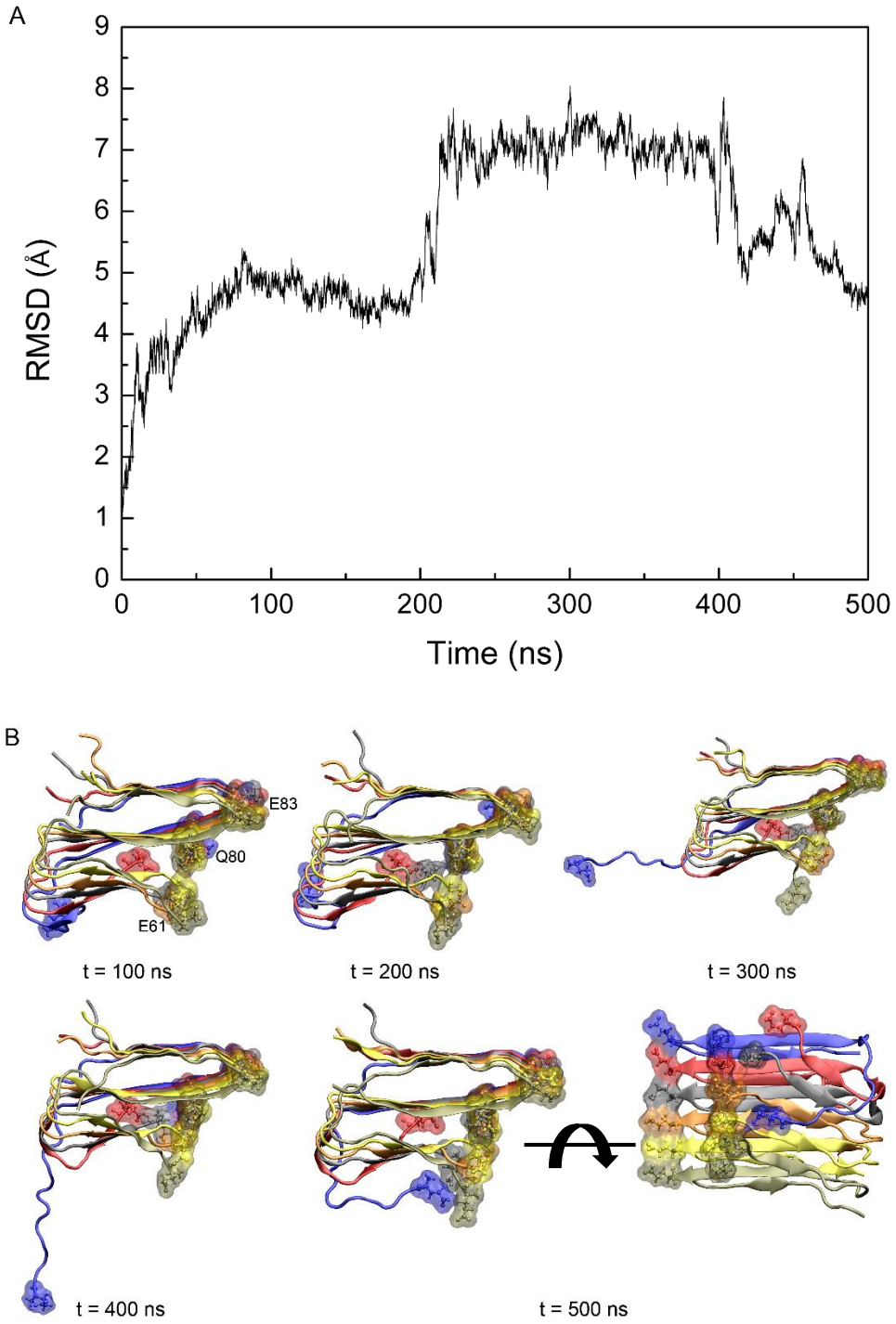

Fig. S7. A second MD simulation of K80Q at 280 K. (A) Computed RMSD timeline. (B) Snapshots at different time steps.

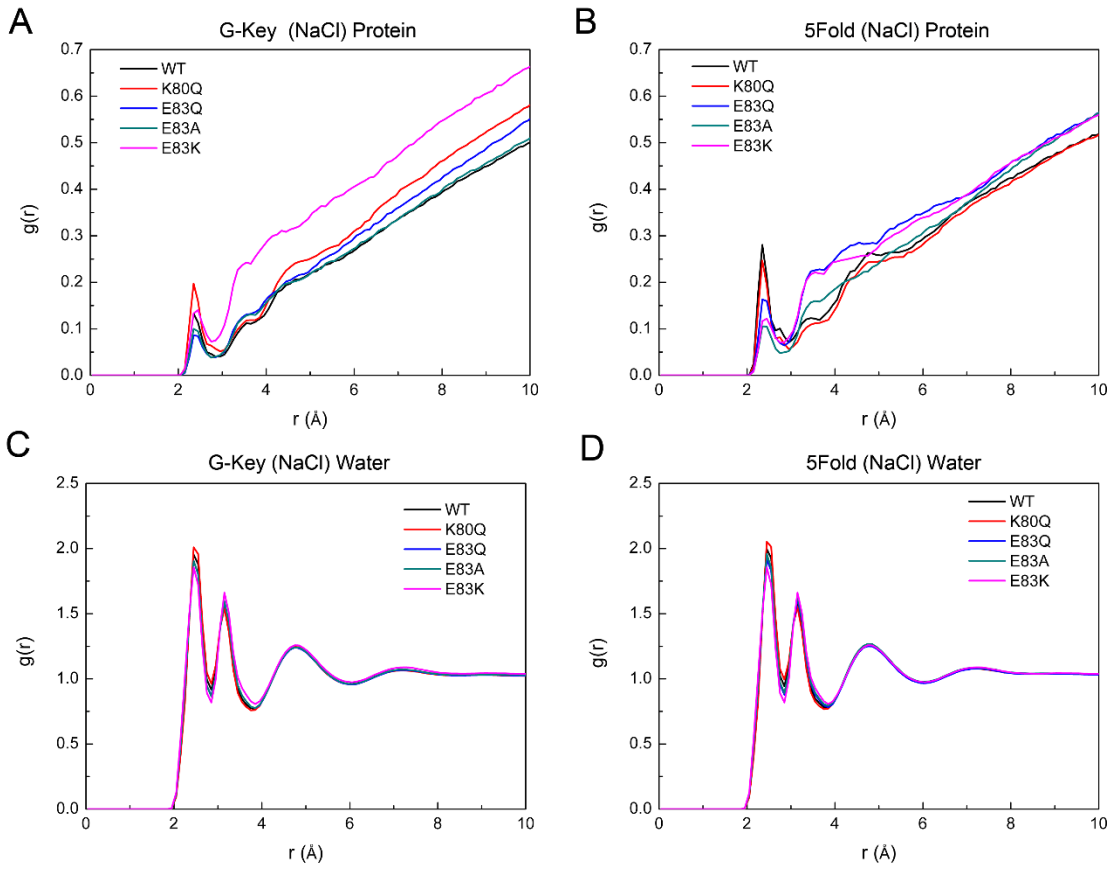

Fig. S8. Radial distribution functions (RDFs) of NaCl-protein and NaCl-water for systems simulated at 310 K in the presence of 0.15 M NaCl.

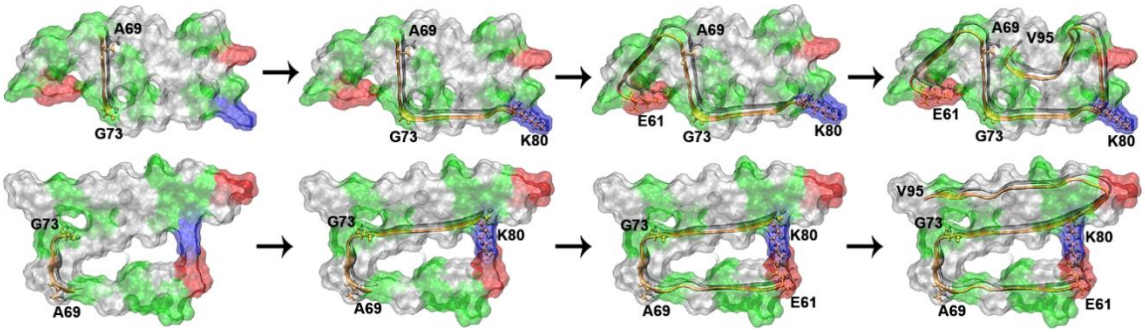

Fig. S9. Proposed assembly pathway using the identified hot spots to form NAC fibrils in different folds sequentially.

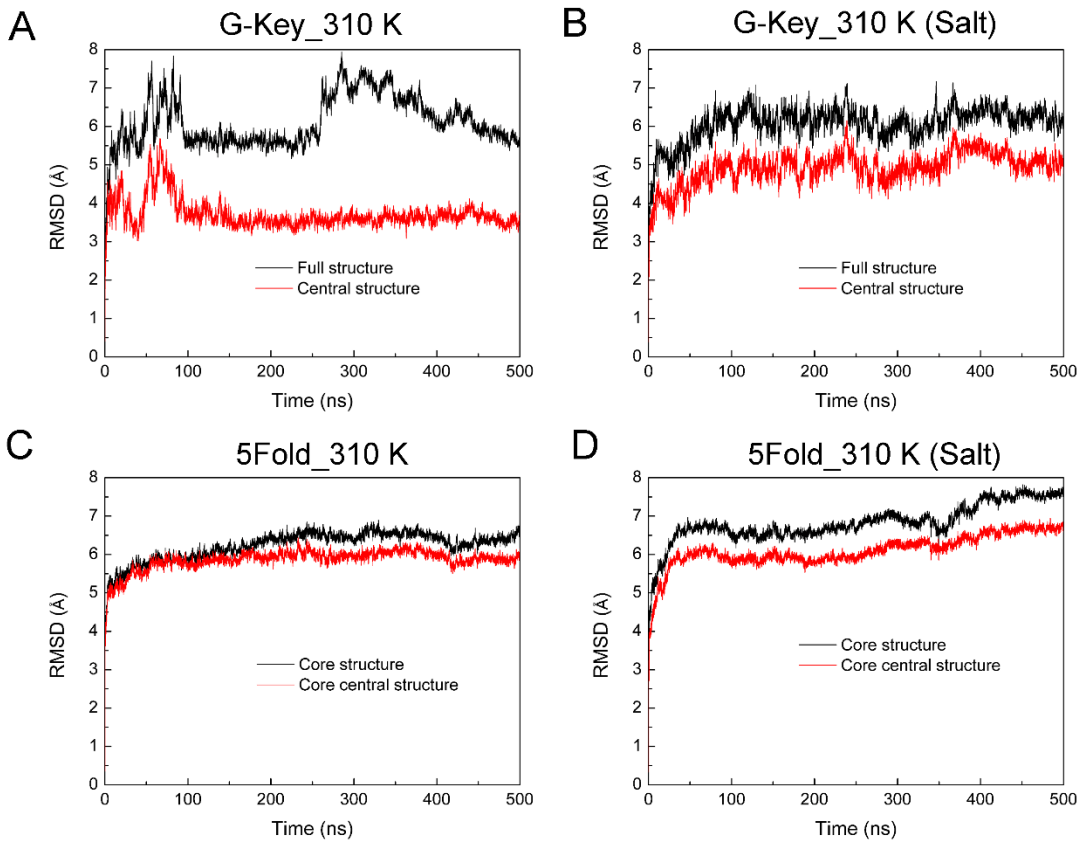

Fig. S10. RMSD of αS fibril core (residues 35–95) in different folds. Core central structure is the corresponding fibril structure without edge monomers.

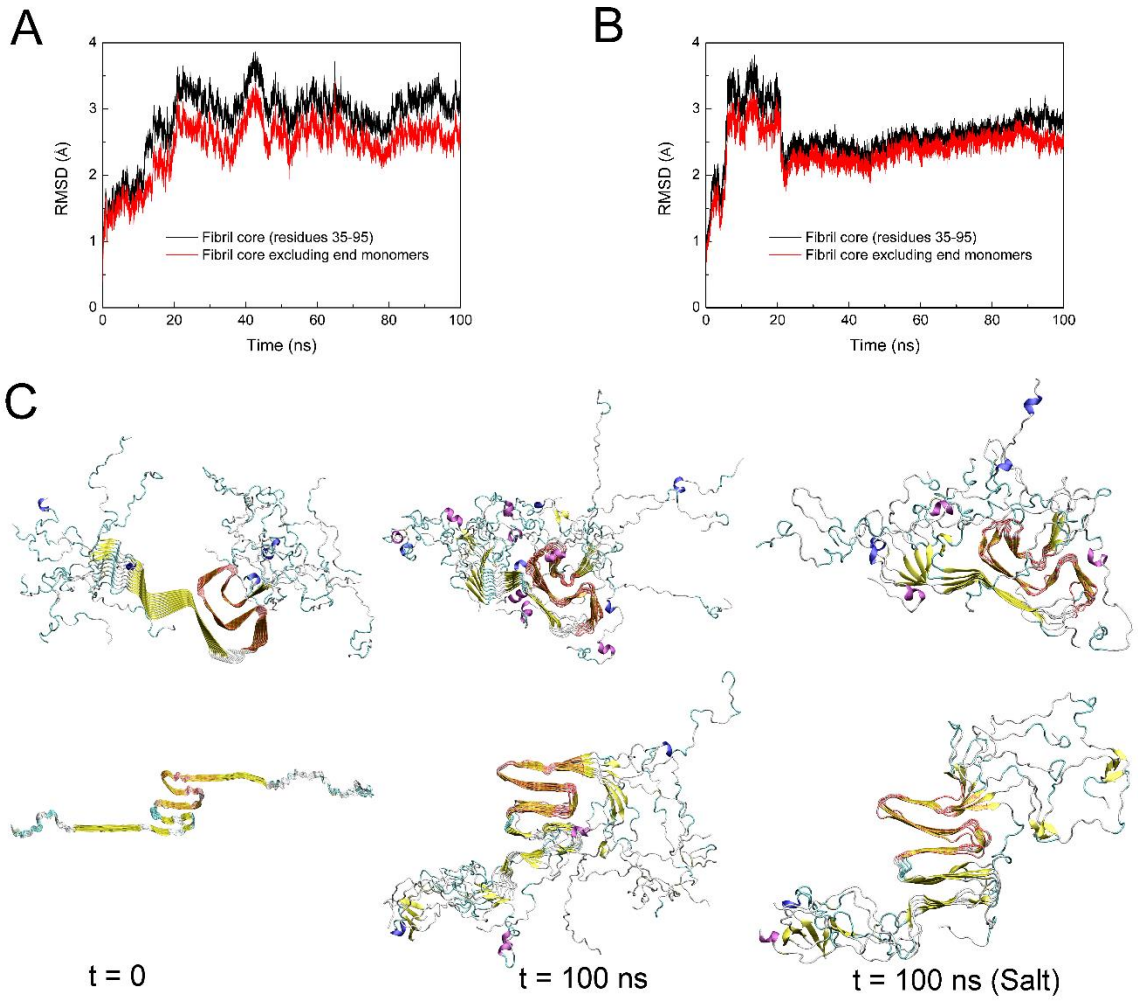

Fig. S11. MD simulations of full-length of αS fibrils in different folds. (A) RMSD over the 100-ns MD simulations of αS fibril in the G-Key fold; (B) RMSD over the 100-ns MD simulations of αS fibril in the five-fold; (C) The starting and final conformations of MD simulations in the absence and presence of 0.15 M NaCl at 310 K. Note that the starting conformations used for MD simulations of fibrils in the 0.15 M NaCl were taken from the final conformations of 100-ns MD simulations of fibrils (decamer) in the absence of NaCl (unpublished data).

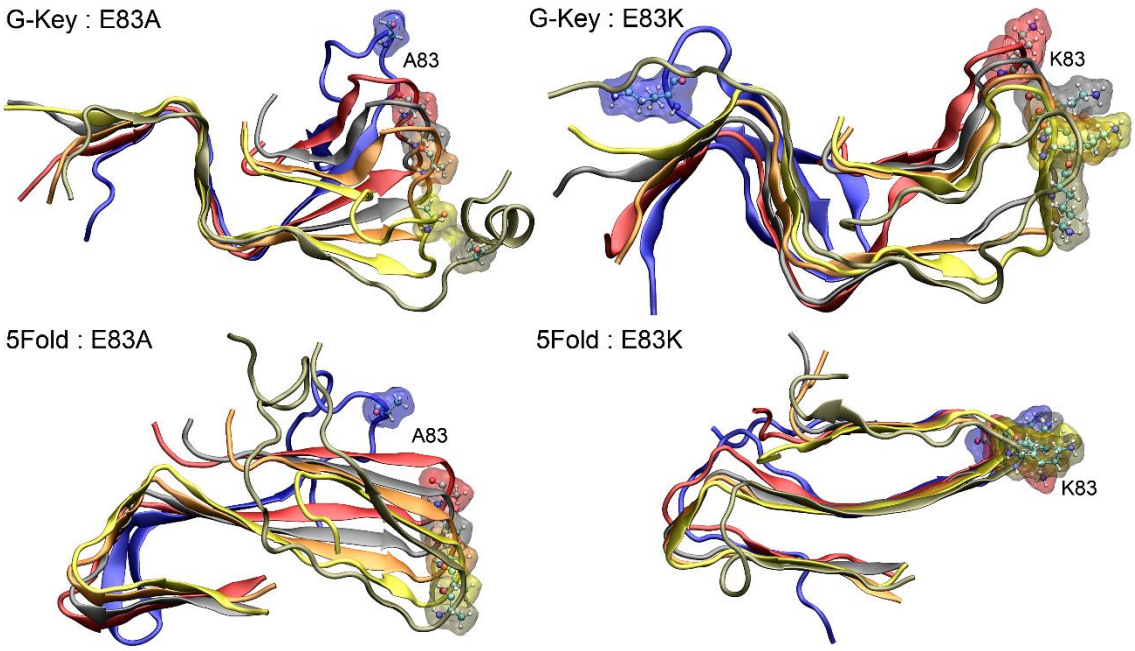

Fig. S12. Final conformations of αS fibril mutants E83A and E83K in both G-Key and 5Fold morphologies. Each simulation was run for 1 μs at 310 K and in the presence of 0.15 M NaCl.

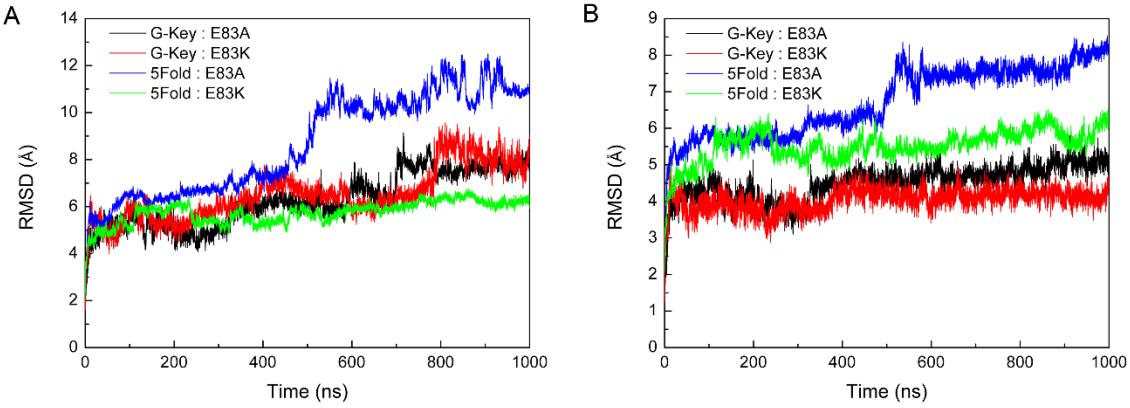

Fig. S13. RMSD of backbone atoms of αS NAC fibril mutants E83A and E83K in both G-Key and 5Fold morphologies. Each simulation was run for 1 μs in the presence of 0.15 M NaCl at 310 K. (A) Backbone atoms of all chains of αS mutants; (B) Backbone atoms of central chains of αS mutants.

Table S1. Comparison of conformational energy (in kcal/mol) for different systems averaged at different time intervals.

System	Last 100 ns of 1-μs	Last 100 ns of 1.5/2.0-μs
G-Key_WT_280 K	-3764 ± 6	-3764 ± 3
G-Key_K80Q_310 K (Salt)	-4088 ± 5	-4094 ± 2
G-Key_E83Q_310 K	-3564 ± 6	-3563 ± 2
5Fold_WT_310 K (Salt)	-3655 ± 7	-3656 ± 4[a]

[a] Conformational energy was averaged over the last 100 ns of 2-μs MD simulations.

Table S2. Average percentage of in-register HBs in different regions of NAC fibrils

	System	Time (ns)	% of in-register HBs in different regions		
G-Key	**WT**		I (Edge A)	II (Central)	III (Edge F)
	280 K	0–500	76±10	75±7	73±10
		500–1000	67±7	71±5	57±8
	310 K	0–500	73±8	83±5	64±15
		500–1000	71±8	84±5	54±8
	310 K, 0.15 M NaCl	0–500	73±11	72±7	69±10
		500–1000	70±8	65±5	58±8
	K80Q				
	280 K	0–500	78±9	83±4	80±8
		500–1000	72±8	86±5	82±8
	310 K	0–500	74±10	91±5	93±11
		500–1000	72±8	89±5	93±9
	310 K, 0.15 M NaCl	0–500	85±10	93±6	73±13
		500–1000	69±11	88±5	44±8
	E83Q				
	280 K	0–500	67±10	88±6	51±13
		500–1000	74±9	81±7	36±7
	310 K	0–500	76±10	77±6	51±13
		500–1000	70±9	80±5	47±8
	310 K, 0.15 M NaCl	0–500	57±10	85±6	68±10
		500–1000	65±9	89±5	66±9
	E83A				
	310 K, 0.15 M NaCl	0–500	70±9	71±7	68±10
		500–1000	63±9	78±5	52±9
	E83K				
	310 K, 0.15 M NaCl	0–500	58±7	79±5	59±7
		500–1000	52±9	76±4	53±10
5Fold	**WT**				
	280 K	0–500	73±7	76±4	69±8
		500–1000	72±7	75±4	68±7
	310 K	0–500	72±7	79±4	72±7
		500–1000	78±8	79±5	72±7
	310 K, 0.15 M NaCl	0–500	79±8	84±4	76±10
		500–1000	61±10	82±5	72±8
	K80Q				
	280 K	0–500	67±8	82±5	78±9
		500–1000	65±8	83±4	87±8

310 K	0–500	74±8	92±5	85±11
	500–1000	74±8	90±5	82±9
310 K, 0.15 M NaCl	0–500	61±9	71±4	71±9
	500–1000	54±5	70±4	71±10
E83Q				
280 K	0–500	74±7	77±4	68±8
	500–1000	71±7	78±4	65±7
310 K	0–500	76±7	80±4	60±9
	500–1000	75±9	82±5	55±6
310 K, 0.15 M NaCl	0–500	76±8	80±4	58±7
	500–1000	76±9	84±4	62±6
E83A				
310 K, 0.15 M NaCl	0–500	35±10	79±6	55±12
	500–1000	32±6	82±4	40±6
E83K				
310 K, 0.15 M NaCl	0–500	76±8	74±5	67±8
	500–1000	60±8	75±4	72±8

Table S3. The population of salt bridges between residues Glu^{61} and Lys^{80} in wild type and E83Q fibrils. A salt bridge is considered to be formed if the distance between any oxygen atom of Glu^{61} and any nitrogen atom of Lys^{80} is ≤3.2 Å in at least one frame of 1-μs MD simulations.

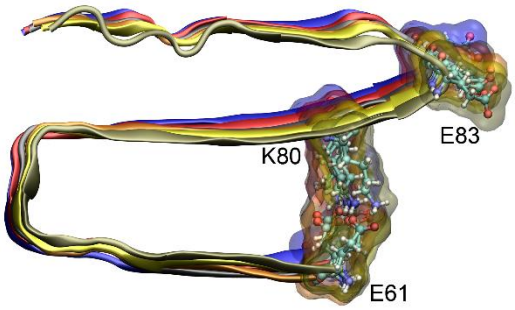

System	Percentage (%)
5Fold_WT_280 K	2
5Fold_WT_310 K	1
5Fold_WT_310 K (0.15 M NaCl)	1
5Fold_E83Q_280 K	1
5Fold_E83Q_310 K	1
5Fold_E83Q_310 K (0.15 M NaCl)	1

Table S4. The conformational energy of αS fibril core and full-length fibrils in different folds.

System		Conformational energy (kcal/mol)	Solvation energy (kcal/mol)
		G-Key	
Core [a]	WT, 310 K	-5777 ± 5	-4908 ± 75
	WT, 310 K, 0.15 M NaCl	-5726 ± 25	-5626 ± 5
Full-length	WT, 310 K [b]	-31639 ± 43	-54686 ± 1920
	WT, 310 K, 0.15 M NaCl [c]	-15481 ± 10	-28685 ± 48
		5Fold	
Core	WT, 310 K	-5741 ± 4	-5065 ± 73
	WT, 310 K, 0.15 M NaCl	-5703 ± 13	-4745 ± 17
Full-length	WT, 310 K[b]	-30259 ± 12	-96567 ± 5905
	WT, 310 K, 0.15 M NaCl [c]	-15414 ± 10	-42457 ± 70

Notes: [a] αS fibril core contains residues 35–95. MD simulations were performed using the same force field parameters as described in the main text.

[b] The full-length αS fibril contains residues 1–140. MD simulations of full-length decamers were performed using the same methods as described in our previous work (*Eur. J. Med. Chem.*, 2016, 121:841). That is, MD simulations were performed using CHARMM27 force field and NAMD 2 software. The solvation energy of full-length αS fibril was calculated using the GBMV method implemented in CHARMM program.

[c] The starting conformations for MD simulations of the full-length αS fibrils (hexamer) in the presence of 0.15 M NaCl were taken from the last frame of 100-ns MD simulations of αS fibrils (decamer, unpublished data). Representative conformations were shown in **Fig. S11**. Different contributions to the conformational energy of the full-length αS fibrils (hexamer) in the presence of 0.15 M NaCl were summarized in **Table S5**.

Table S5. The conformational energy (and individual contributions) of full-length αS fibrils in different folds. MD simulations were performed in the presence of 0.15 M NaCl and at 310 K. Energy unit: kcal/mol.

	G-Key (kcal/mol)	**5Fold (kcal/mol)**
MM_Electrostatic	703 ± 40	14543 ± 58
MM_vdW	-2064 ± 7	-2096 ± 7
MM_Bonded	14565 ± 8	14596 ± 5
MM_Total	13205 ± 39	27043 ± 60
GB_Polar	-28951 ± 50	-42725 ± 72
GB_Nonpolar	266 ± 2	268 ± 2
GB_Solvation	-28685 ± 48	-42457 ± 70
Total Electrostatic	-28248 ± 10	-28182 ± 14
MM_GBSA (Conformational energy)	-15481 ± 10	-15414 ± 10

Table S6. Conformational energy of NAC fibrils bearing E83 mutations and water diffusion constant on fibril surface. All simulations were under the same condition: 310 K and the presence of 0.15 M NaCl.

E83 mutant	**Conformational energy (kcal/mol)**	**Solvation energy (kcal/mol)**	**Water diffusion constant (10^{-5} cm^2/s)**
		G-Key	
E83A	-3106 ± 10	-2048 ± 5	2.5 ± 0.1
E83K	-3176 ± 2	-2912 ± 51	2.6 ± 0.1
E83Q	-3598 ± 1	-2360 ± 8	2.7 ± 0.0
		5Fold	
E83A	-3088 ± 17	-1934 ± 39	2.4 ± 0.0
E83K	-3121 ± 12	-2990 ± 54	2.5 ± 0.0
E83Q	-3560 ± 2	-2073 ± 5	2.2 ± 0.3